

Unstable modes of hypermassive compact stars driven by viscosity and gravitational radiation

Peter B. Rau¹^{*} and Armen Sedrakian^{2,3}[†]

¹*Cornell Center for Astrophysics and Planetary Science and Department of Astronomy, Cornell University, Ithaca, NY 14850, U.S.A.*

²*Frankfurt Institute for Advanced Studies, D-60438 Frankfurt am Main, Germany*

³*Institute of Theoretical Physics, University of Wrocław, 50-204 Wrocław, Poland*

Accepted XXXX. Received XXXX; in original form XXXX

ABSTRACT

We study the oscillations modes of differential rotating remnants of binary neutron star inspirals by modeling them as incompressible Riemann ellipsoids parametrized by the ratio f of their internal circulation to the rotation frequency. The effects of viscosity and gravitational wave radiation on the modes are studied and it is shown that these bodies exhibit generic instabilities towards gravitational wave radiation akin to the Chandrasekhar–Friedman–Schutz instabilities for uniformly rotating stars. The odd-parity modes are unstable for all values of f (except for the spherical model) and deformations, whereas the even parity unstable modes appear only in highly eccentric ellipsoids. We quantify the modification of the modes with varying mass of the model and the magnitude of the viscosity. The modes are weakly dependent on the range of the masses relevant to the binary neutron star mergers. Large turbulent viscosity can lead to a suppression of the gravitational wave instabilities, whereas kinematical viscosity has a negligible influence on the modes and their damping timescales.

Key words: stars: neutron – stars: oscillations – instabilities – gravitational waves

1 INTRODUCTION

Hypermassive neutron stars (HMNS) are one of the possible outcomes of binary neutron star (BNS) mergers. They are characterized as having a mass greater than the maximum value for a uniformly rotating neutron star, but are supported against gravitational collapse by the differential motion of their interior fluids. Numerical simulations (for recent examples, see [Kastaun & Galeazzi \(2015\)](#); [Kastaun et al. \(2017\)](#); [Dietrich et al. \(2017\)](#); [Radice et al. \(2018\)](#); [Most et al. \(2019\)](#); [Hanauske et al. \(2019\)](#); [Ruiz et al. \(2020\)](#); [Chaurasia et al. \(2020\)](#)) show that after a period of ~ 10 ms of nonlinear evolution, post-merger objects settle into equilibria supported against collapse by differential rotation. These equilibria can be highly eccentric and emit gravitational radiation that could be detected by gravitational wave interferometers ([LIGO Scientific Collaboration and Virgo Collaboration: et al. 2019](#)). Depending on its mass, an HMNS may eventually collapse to a black hole or evolve to a supramassive, uniformly rotating, compact star. Supramassive neutron stars (SMNS), which have masses exceeding the maximum value for a nonrotating star, evolve by losing angular momentum into stable neutron stars or collapse to black holes, depending on whether their lower-spin counterparts along the constant baryon mass sequence belong to a stable or unstable branch.

Two merger events, GW170817 ([LIGO Scientific Collaboration and Virgo Collaboration: et al. 2017](#)) and GW190425 ([LIGO Sci-](#)

[entific Collaboration and Virgo Collaboration: et al. 2021](#)), observed by the LIGO–Virgo collaboration, have definite BNS origin. The combined masses of merged stars are $2.74M_{\odot}$ and $3.4M_{\odot}$ respectively. Whether or not these mergers resulted in a prompt collapse to a black hole or led to the formation of an HMNS is still an open question, but the electromagnetic follow-up emission to GW170817 suggests that a short-lived HMNS was formed ([Shibata et al. 2017](#); [Margalit & Metzger 2017](#); [Bauswein et al. 2017](#); [Gill et al. 2019](#)). Given the detection rate of compact binary coalescence of one per week at the current LIGO–Virgo collaboration sensitivity, the prospect of observing BNS mergers in the future is optimistic.

The Fourier analysis of the gravitational wave spectrum emitted by an HMNS in numerical simulations shows clear peaks at frequencies in the range 1–4 kHz ([Bauswein et al. 2014](#); [Takami et al. 2014](#); [Stergioulas et al. 2011](#)). Their physical origin is obscured by the complex fluid dynamics of HMNS in this “ring-down” phase. These frequencies could be visible to advanced LIGO if the BNS merger is close enough (at distances of the order of 40 Mpc) and other more sensitive telescopes, such as the Einstein Telescope ([Maggiore et al. 2020](#)) and the Cosmic Explorer ([Reitze et al. 2019](#)) in a more distant future. Apart from the detection perspective, understanding the oscillation spectrum and the stability of HMNS is important for assessing their lifetimes, mechanism of collapse, and spectrum of oscillations on longer (of the order of 10–100 ms) time scales. Because of the high computational cost of running BNS simulations on such timescales and the complexity of implementing viscosity in full-scale numerical simulations, studies of quasinormal modes of HMNS using semi-analytic methods are useful both for covering large parameter spaces as well as gaining insights in the physics of the oscillations and instabilities.

^{*} E-mail: prau@uw.edu (Corresponding author. Current address: Institute for Nuclear Theory, University of Washington, Seattle, WA 98195-4550, U.S.A.)

[†] E-mail: sedrakian@fias.uni-frankfurt.de

Uniformly rotating gravitationally-bound stars (as first demonstrated for ellipsoidal bodies by Chandrasekhar (1969), hereafter abbreviated as EFE) undergo secular instabilities induced by viscosity (Roberts & Stewartson 1963; Rosenkilde 1967) and gravitational radiation (Chandrasekhar 1970). These instabilities appear both in Newtonian and general-relativistic setting and for realistic equations of states, which indicates that they are generic in compact stars. The importance of the Chandrasekhar–Friedmann–Schutz (CFS) instability (Chandrasekhar 1970; Friedman & Schutz 1978) to gravitational wave-radiation in rotating stars, in particular, its manifestation in the r -mode instability (for reviews see Kokkotas & Schwenzer (2016); Andersson (2021)), lies in the fact that they may set an upper limit on rotational periods of a rapidly rotating compact stars.

In a previous paper (Rau & Sedrakian 2020) we showed that *Riemann ellipsoids* – non-axisymmetric self-gravitating Newtonian fluid bodies with constant internal circulation – undergo secular instabilities driven by gravitational wave radiation or by viscosity (note, however, that viscosity alone may drive secular instability (Rosenkilde 1967)). Because these ellipsoids possess, in general, a non-vanishing fluid pattern in the frame rotating with its surface, they can be viewed as (approximate) models of differentially-rotating HMNS. Although more complex models which include post-Newtonian corrections (Chandrasekhar & Elbert 1974; Shapiro & Zane 1998; Gürlebeck & Petroff 2010, 2013), full relativity or realistic equations of state can be constructed, it is useful to first establish the key features in the classical framework of ellipsoids, as exemplified by the cases without internal circulation by Chandrasekhar (1969).

In this paper, we provide a detailed description of the formalism and extended computations within the approach adopted in Rau & Sedrakian (2020). In particular, we focus on the unstable modes of Riemann S-type ellipsoids including gravitational radiation and shear viscosity. In doing so we find the modes for multiple stellar masses and various choices of shear viscosity. While in Rau & Sedrakian (2020) we studied secularly unstable modes of $2.74M_{\odot}$, uniform density Riemann S-type ellipsoids, in this paper we cover a range of masses between $2M_{\odot}$, corresponding to a neutron star below the maximum mass at which collapse to a black hole is inevitable, up to $3.5M_{\odot}$, which is roughly at the mass limit for prompt collapse to a black hole. We also examine a range of (shear) viscosities, which includes “enhanced” values (aimed to mimic the effect of putative turbulent viscosity) which lead to dissipation comparable to the gravitational radiation damping. We assume that HMNS are sufficiently hot so that the superfluidity of baryonic matter which arises at low temperatures can be neglected; otherwise one needs to minimally account for the two-fluid nature of matter and for superfluid effects such as mutual friction, which can be included in the formalism adopted here [see Sedrakian & Wasserman (2001)].

The non-dissipative modes of oscillations of Riemann ellipsoids were already derived in EFE. However, subsequent work on Riemann ellipsoids focused on a different problem – the modeling of the secular evolution of differentially-rotating stars under the action of gravitational radiation and (shear) viscosity. Clearly, Riemann ellipsoids undergo unstable evolution of their triaxial shape due to gravitational radiation. Press & Teukolsky (1973) showed, through numerical integration of the equations of motion which included viscosity of the fluid, that secular instability drives a Maclaurin spheroid into a stable Jacobi ellipsoid via intermediate states which are Riemann S-type ellipsoids. The equations of motion of Riemann S-type ellipsoids under gravitational radiation-reaction were later integrated by Miller (1974) and it was shown that they again evolve into bodies with vanishing internal circulation with or without axial symmetry. The combined effect of viscosity and gravitational radiation was first con-

sidered by Detweiler & Lindblom (1977) and further extended by Lai & Shapiro (1995) to the compressible ellipsoidal approximation (Lai et al. 1993) to obtain insights into the evolution of a secularly unstable newly-born neutron star. The dissipative modes of Riemann ellipsoids were derived only recently (Rau & Sedrakian 2020); here we provide an extended discussion of the underlying formalism and a parameter study, which complements our earlier discussion (Rau & Sedrakian 2020).

Section 2 describes the tensor-virial formalism used to find the gravitational radiation-unstable modes and determine the effects of viscosity on them. Section 3 discusses the numerical results, by first comparing the unstable mode growth times for different masses of models, and then for a range of viscosity values. The results are summarized in Section 4. The gravitational wave back-reaction terms and characteristic equations used to compute the modes are given in full detail in Appendices A and B respectively. In Appendix C we provide the full 2.5-post-Newtonian gravitational radiation back-reaction terms for Riemann S-type ellipsoids, though as we discuss later on, only the limiting expressions given in Appendix A are used for numerical computations.

2 PERTURBATION EQUATIONS FROM THE TENSOR-VIRIAL FORMALISM

The theory of the equilibrium ellipsoids and their oscillations is summarized by Chandrasekhar in EFE. We now briefly review the formalism used in the previous work (Rau & Sedrakian 2020), which is based on EFE, and include below explicitly some of the equations which were left out from this work for brevity.

We consider the perturbations of triaxial Riemann S-type ellipsoids i.e. ellipsoids with principal axes $a_1 \neq a_2 \neq a_3$. The principal axes are at rest in a corotating frame, which has angular velocity $\Omega = \Omega(t)$ with respect to the inertial frame, and which has internal motions with uniform vorticity ω as measured in the corotating frame. It is assumed that ω and Ω are parallel, and are chosen to lie along the $z = x_3$ axis, which is the same in the inertial and corotating frames. Without loss of generality we take $a_1 \geq a_2$. We consider incompressible flows $\nabla \cdot \xi = 0$, where ξ is the Lagrangian displacement, and assume uniform density for simplicity. For perturbations with Lagrangian displacement of the form

$$\xi(\mathbf{x}, t) = e^{i\lambda t} \xi(\mathbf{x}), \quad (1)$$

the second-order tensor-virial equation leads to the characteristic equations (including viscosity and gravitational radiation back-reaction) given by (see also EFE)

$$\begin{aligned} & \lambda^2 V_{i,j} - 2\lambda Q_{jl} V_{i;l} - 2\lambda \Omega \epsilon_{i\ell 3} V_{\ell;j} \\ & - 2\Omega \epsilon_{i\ell 3} (Q_{\ell k} V_{j;k} - Q_{jk} V_{\ell;k}) + Q_{j\ell}^2 V_{i;\ell} + Q_{i\ell}^2 V_{j;\ell} \\ = & \Omega^2 (V_{ij} - \delta_{i3} V_{3j}) + \delta \mathfrak{B}_{ij} + \delta_{ij} \delta \Pi - \delta \mathfrak{P}_{ij} - \delta \mathcal{G}_{ij}, \end{aligned} \quad (2)$$

where the Latin indices $i, j = 1, 2, 3$ are the components of the Cartesian coordinate system. This is a set of nine equations for $V_{i,j}$ and $V_{i,j}$, which are the unsymmetrized and symmetrized perturbations of the quadrupole moment tensor

$$V_{i;j} = \int_{\mathcal{V}} d^3 x \rho \xi_i x_j \quad V_{ij} = \int_{\mathcal{V}} d^3 x \rho (\xi_i x_j + x_i \xi_j), \quad (3)$$

where ρ is the density of the star, x_i the coordinates in the rotating frame and \mathcal{V} the volume of the ellipsoid. The matrices Q_{ij} relate the background flow velocity inside the star u_i to the coordinates in the rotating frame x_j

$$u_i = Q_{ij} x_j, \quad (4)$$

where for the case of the Riemann S-type ellipsoids and with $\mathbf{\Omega}$ and ω aligned with the x_3 axis we have

$$u_1 = Q_{12}x_2, \quad Q_{12} = -\frac{a_1^2}{a_1^2 + a_2^2}\Omega f, \quad (5)$$

$$u_2 = Q_{21}x_1, \quad Q_{21} = \frac{a_2^2}{a_1^2 + a_2^2}\Omega f, \quad (6)$$

$$u_3 = 0, \quad (7)$$

and all other elements of Q_{ij} equal to zero. The differential rotation is parametrized in terms of the quantity $f \equiv \omega/\Omega$, where ω and Ω are the magnitudes of ω and $\mathbf{\Omega}$. The different Riemann sequences are labeled by their value of f , with $f = 0$ being the (*uniformly rotating*) Jacobi ellipsoids and $f = \pm\infty$ being the Dedekind ellipsoids (for details see EFE). The case $f = -2$ corresponds to an irrotational ellipsoid since the vorticity in the inertial frame is given by $\omega_0 = (2 + f)\mathbf{\Omega}$. In Eq. (2) $\delta\mathfrak{B}_{ij}$ denotes the gravitational potential energy tensor given by

$$\delta\mathfrak{B}_{ij} = -\int_{\mathcal{V}} d^3x \rho \xi_\ell \frac{\partial \mathfrak{B}_{ij}}{\partial x_\ell}, \quad (8)$$

where \mathfrak{B}_{ij} is defined such that

$$\frac{\partial \mathfrak{B}_{ij}}{\partial x_\ell} = -\delta_{i\ell} \frac{\partial \mathfrak{B}}{\partial x_j} - \delta_{j\ell} \frac{\partial \mathfrak{B}}{\partial x_i} - 3\mathfrak{B}_{ij\ell}, \quad (9)$$

and where

$$\frac{\partial \mathfrak{B}}{\partial x_i} = -G \int_{\mathcal{V}} d^3x \rho(\mathbf{x}') \frac{x_i - x'_i}{|\mathbf{x} - \mathbf{x}'|^3}, \quad (10)$$

$$\mathfrak{B}_{ij\ell} = G \int_{\mathcal{V}} d^3x \rho(\mathbf{x}') \frac{(x_i - x'_i)(x_j - x'_j)(x_\ell - x'_\ell)}{|\mathbf{x} - \mathbf{x}'|^5}, \quad (11)$$

where G is Newton's constant. For a homogeneous star, EFE gives

$$\mathfrak{B}_{ij} = \pi G \rho \left[2B_{ij}x_ix_j + a_i^2 \delta_{ij} \left(A_i - \sum_{\ell=1}^3 A_{i\ell} x_\ell^2 \right) \right], \quad (12)$$

where the index symbols A_{ij} and B_{ij} are defined as

$$A_{ij} = a_1 a_2 a_3 \int_0^\infty \frac{du}{\Delta(u)(a_i^2 + u)(a_j^2 + u)}, \quad (13)$$

$$B_{ij} = a_1 a_2 a_3 \int_0^\infty \frac{udu}{\Delta(u)(a_i^2 + u)(a_j^2 + u)}, \quad (14)$$

$$\Delta(u) \equiv \sqrt{(a_1^2 + u)(a_2^2 + u)(a_3^2 + u)}. \quad (15)$$

It follows that in the homogeneous case Eq. (8) gives

$$\delta\mathfrak{B}_{ij} = -\pi G \rho \left[2B_{ij}V_{ij} - \delta_{ij} a_i^2 \sum_{\ell=1}^3 A_{i\ell} V_{\ell\ell} \right]. \quad (16)$$

Finally, $\delta\Pi$ In Eq. (2) is the Eulerian perturbation of the volume integral of the pressure, i.e.,

$$\delta\Pi = -\int_{\mathcal{V}} d^3x (\gamma - 1) P \frac{\partial \xi_k}{\partial x_k}, \quad (17)$$

where $P = P(\mathbf{x})$ is the pressure and γ is the ratio of specific heats. For incompressible flows, we must first eliminate $\delta\Pi$ from the virial characteristic equations and only then impose incompressibility.

The Eulerian perturbation of viscous stress tensor $\delta\mathfrak{P}_{ij}$ for an

incompressible fluid with a background velocity u_k is

$$\begin{aligned} \delta\mathfrak{P}_{ij} = \int_{\mathcal{V}} d^3x \rho \nu \left[\lambda \left(\frac{\partial \xi_i}{\partial x_j} + \frac{\partial \xi_j}{\partial x_i} \right) + \frac{\partial \xi_i}{\partial x_k} \frac{\partial u_k}{\partial x_j} \right. \\ \left. + \frac{\partial \xi_j}{\partial x_k} \frac{\partial u_k}{\partial x_i} + u_k \left(\frac{\partial^2 \xi_i}{\partial x_k \partial x_j} + \frac{\partial^2 \xi_i}{\partial x_k \partial x_j} \right) \right. \\ \left. - \frac{\partial \xi_k}{\partial x_j} \frac{\partial u_i}{\partial x_k} - \frac{\partial \xi_k}{\partial x_i} \frac{\partial u_j}{\partial x_k} \right] \end{aligned} \quad (18)$$

where ν is the kinematic shear viscosity coefficient. We note that in [Rau & Sedrakian \(2020\)](#) we kept only the the first term in the integrand and thus neglected (erroneously) additional terms due to internal rotation; we keep these terms here and verify that the results reported in [Rau & Sedrakian \(2020\)](#) are unchanged qualitatively. Below we work in the low Reynolds number approximation i.e. the laminar flow regime for which the displacement fields for the inviscid flow are essentially unchanged when viscosity is included. This implies that we can use as the eigenfunctions ξ in the absence of viscosity

$$\xi_i = \sum_{m=1}^3 L_{i;m} x_m, \quad (19)$$

when evaluating the perturbations of the viscous stress tensor; here the $L_{i;m}$ are nine constants determined in the non-dissipative limit. Inserting this into Eq. (18) and using Eq. (4) gives

$$\begin{aligned} \delta\mathfrak{P}_{ij} = 5\nu \left[\lambda \left(\frac{V_{i;j}}{a_j^2} + \frac{V_{j;i}}{a_i^2} \right) + Q_{kj} \frac{V_{i;k}}{a_k^2} - Q_{jk} \frac{V_{k;i}}{a_i^2} \right. \\ \left. + Q_{ki} \frac{V_{j;k}}{a_k^2} - Q_{ik} \frac{V_{k;j}}{a_j^2} \right]. \end{aligned} \quad (20)$$

Note that Eq. (19) implies that for incompressible flows

$$\frac{V_{11}}{a_1^2} + \frac{V_{22}}{a_2^2} + \frac{V_{33}}{a_3^2} = 0. \quad (21)$$

According to Appendix A, the gravitational radiation back-reaction term $\delta\mathcal{G}_{ij}$ is

$$\delta\mathcal{G}_{ij} = \frac{2G}{5c^5} \left(\dot{I}_{i\ell}^{(5)} V_{\ell j} + \dot{I}_{\ell i}^{(5)} I_{\ell j} \right), \quad (22)$$

where $\dot{I}_{ij}^{(5)}$ is the fifth time derivative of the reduced quadrupole moment tensor of the ellipsoid in the inertial frame projected onto the rotating frame, defined in terms of the quadrupole moment tensor as

$$\dot{I}_{ij}^{(5)} = I_{ij}^{(5)} - \frac{1}{3} \delta_{ij} \text{Tr}(I^{(5)}), \quad (23)$$

where ([Chandrasekhar & Esposito 1970](#); [Miller 1974](#))

$$I_{ij}^{(5)} = \sum_{m=0}^5 \sum_{p=0}^m C_m^5 C_p^m (-1)^p [(\bar{\mathbf{\Omega}}^*)^p]_{ik} \frac{d^{5-m} I_{k\ell}^{(r)}}{dt^{5-m}} [(\bar{\mathbf{\Omega}}^*)^{m-p}]_{\ell j}. \quad (24)$$

$I_{k\ell}^{(r)}$ is the moment of inertia tensor in the rotating frame, C_n^m are binomial coefficients, and for rotation about the x_3 axis, the matrix $\bar{\mathbf{\Omega}}^*$ takes the form

$$\bar{\mathbf{\Omega}}^* = \begin{pmatrix} 0 & \Omega & 0 \\ -\Omega & 0 & 0 \\ 0 & 0 & 0 \end{pmatrix} \equiv \mathbf{\Omega} \sigma, \quad (25)$$

which defines the matrix σ . For a time-independent moment of inertia as measured in the rotating frame, Eq. (24) reduces to

$$I_{ij}^{(5)} = \sum_{p=0}^5 C_p^5 (-1)^p [(\bar{\Omega}^*)^p]_{ik} I_{k\ell}^{(r)} [(\bar{\Omega}^*)^{5-p}]_{\ell j}. \quad (26)$$

For a triaxial ellipsoid in the rotating frame, where the principal axes are aligned with the coordinate axes, $I_{ij} = I_{ij}^{(r)}$ is

$$I_{ij} = \frac{1}{5} M \delta_{ij} \left(\sum_{m=1}^3 a_m^2 - a_i^2 \right). \quad (27)$$

We further use the expression for $I_{ij}^{(5)}$ given in the appendix of [Lai et al. \(1994\)](#). Since Ω and I_{ij} are constant in time, the only nonzero component of $I_{ij}^{(5)}$ is

$$I_{12}^{(5)} = I_{21}^{(5)} = 16\Omega^2 (I_{11} - I_{22}). \quad (28)$$

Analogously to $I_{ij}^{(5)}$ one finds for $V_{ij}^{(5)}$

$$V_{ij}^{(5)} = V_{ij}^{(5)} - \frac{1}{3} \delta_{ij} \text{Tr}(V^{(5)}), \quad (29)$$

where

$$\begin{aligned} V_{ij}^{(5)} &= \sum_{m=0}^5 \sum_{p=0}^m C_m^5 C_p^m (-1)^p [(\bar{\Omega}^*)^p]_{ik} \frac{d^{5-m} V_{k\ell}}{dt^{5-m}} [(\bar{\Omega}^*)^{m-p}]_{\ell j} \\ &= \lambda^5 V_{ij} - 20\lambda\Omega^2 (\lambda^2 - 2\Omega^2) (V_{ik}(\sigma^4)_{kj} + \sigma_{ik} V_{k\ell} \sigma_{\ell j}) \\ &\quad + \Omega (5\lambda^4 - 40\lambda^2\Omega^2 + 16\Omega^4) (V_{ik}\sigma_{kj} - \sigma_{ik} V_{kj}) \\ &= \lambda^5 V_{ij} - \phi_1(\lambda, \Omega) (V_{ik}(\sigma^4)_{kj} + \sigma_{ik} V_{k\ell} \sigma_{\ell j}) \\ &\quad + \phi_2(\lambda, \Omega) (V_{ik}\sigma_{kj} - \sigma_{ik} V_{kj}), \end{aligned} \quad (30)$$

where we used the time-dependence of ξ from Eq. (1) and defined the auxiliary functions

$$\phi_1(\lambda, \Omega) \equiv 20\lambda\Omega^2 (\lambda^2 - 2\Omega^2), \quad (31)$$

$$\phi_2(\lambda, \Omega) \equiv \Omega (5\lambda^4 - 40\lambda^2\Omega^2 + 16\Omega^4). \quad (32)$$

The $i, j \neq 3$ components of $V_{ij}^{(5)}$ match those of $\delta\mathbf{I}^{(5)}$ given in Eq. (28) of [Chandrasekhar & Esposito \(1970\)](#).

The rotational frequency and the characteristic frequencies can be made dimensionless using

$$\bar{\Omega} \equiv \frac{\Omega}{\sqrt{\pi G \rho}}, \quad \bar{\lambda} \equiv \frac{\lambda}{\sqrt{\pi G \rho}}. \quad (33)$$

The shear viscosity term coefficients are made dimensionless through an additional factor of a_1^{-2} such that the dimensionless kinematic shear viscosity is

$$\begin{aligned} \bar{\nu} &\equiv \frac{\nu}{a_1^2 \sqrt{\pi G \rho}} \\ &= 1.35 \times 10^{-13} \left(\frac{\nu}{10^3 \text{ cm}^2 \text{ s}^{-1}} \right) \left(\frac{\rho_0}{\rho} \right)^{1/2} \left(\frac{10 \text{ km}}{a_1} \right)^2, \end{aligned} \quad (34)$$

where $\rho_0 = 2.7 \times 10^{14} \text{ g/cm}^3$ is nuclear saturation density. The terms describing the damping due to gravitational wave radiation will scale as \bar{t}_c^5 , where \bar{t}_c is the dimensionless light crossing time

$$\bar{t}_c \equiv \frac{a_1 \sqrt{\pi G \rho}}{c} = 0.251 \left(\frac{\rho}{\rho_0} \right)^{1/2} \left(\frac{a_1}{10 \text{ km}} \right). \quad (35)$$

The dependence of $\bar{\nu}$ and \bar{t}_c on the density and the semi-axis length a_1 of the ellipsoid means that the mode frequencies $\bar{\lambda}$ will also depend on these quantities, unlike in the cases where viscosity and gravitational wave damping are absent.

3 NUMERICAL RESULTS

As discussed in [Rau & Sedrakian \(2020\)](#), the procedure to compute the ellipsoid modes first involves determining the sequence of equilibrium Riemann S-type ellipsoids for each value of f using the procedure described in EFE. These sequences consist of values of α , β and $\bar{\Omega}$. A selection of these sequences in the range $-\infty \leq f \leq \infty$ are given in Fig. 1. The mode frequencies are then computed by solving matrix equations formed from the components of the tensorial characteristic equation Eq. (2); these equations are given explicitly in Appendix B.

The components of the characteristic equation, and the resulting mode frequencies, are grouped into even ($ij = 11, 22, 33, 12, 21$) and odd ($ij = 13, 31, 23, 32$) in the index 3 (the x_3 axis is aligned with the spin vector of the ellipsoid). The even modes correspond to toroidal perturbations of the ellipsoid, and the odd modes to transverse-shear perturbations. The even-parity equations result in an order 17 polynomial in $\bar{\lambda}$, and the odd-parity equations in a polynomial of order 14 in $\bar{\lambda}$. However, not all the modes are physically relevant. The reason is that, as in [Rau & Sedrakian \(2020\)](#), we work with Newtonian background ellipsoids and Newtonian equations of motion, therefore we are able to compute the gravitational wave back-reaction effects on the ‘‘perturbative’’ modes only. By this, we mean the modes which differ from the normal non-dissipative modes of the ellipsoid λ_0 by a small correction $\delta\lambda \in \mathbb{C}$, $|\delta\lambda| \ll |\lambda_0|$. Since the equilibrium background upon which perturbations are imposed is Newtonian, it is sufficient to consider the leading post-Newtonian order gravitational-radiation reaction contribution given by Eq. (22). However, in Appendix C, we compute the full 2.5-post-Newtonian gravitational wave back-reaction terms. These can be used to address (some of) the remaining non-perturbative modes by computing the equilibrium background models at a post-Newtonian order. Such a program will allow one to assess the oscillation frequencies and damping of non-perturbative modes.

When discussing the numerical results for perturbative modes we define $\bar{\sigma} = -i\bar{\lambda}$. The unstable perturbative modes are those with $\text{Im}(\sigma) < 0$, and the dimensionless growth time of these modes is specified by

$$\bar{\tau} = -\frac{1}{\text{Im}(\bar{\sigma})}. \quad (36)$$

By definition, $\text{Re}(\sigma)$ provides the oscillation frequency of the mode. We assign, additionally, indices e or o to quantities referring to even or odd modes respectively.

In our previous work ([Rau & Sedrakian 2020](#)) we included unstable modes for a $2.74M_\odot$ ellipsoid (to match the mass of GW170817) with uniform density $\rho = 3.62\rho_0$. In this section we examine a range of stellar masses $2M_\odot < M < 3.5M_\odot$. [Weih et al. \(2018\)](#) gives a threshold mass for prompt collapse as $1.54M_{\text{TOV}}$ for a differentially-rotating star, so for a maximum TOV mass M_{TOV} in line with the highest measured neutron star mass to date of $2.14M_\odot$ ([Cromartie et al. 2020](#)), we should at least consider masses above $\sim 3.3M_\odot$, and thus choose an upper mass range of $3.5M_\odot$. For each model, we set the uniform density ρ by enforcing that the $f = -2$, $\alpha = \beta = 1$ star has a radius of $a_1 = 11 \text{ km}$. For every other ellipsoid for a particular fixed mass, we adjust a_1 so that each ellipsoid has constant volume, and hence the same mass. The six stellar models examined in the next two sections, and their uniform densities, are listed in Table 1.

3.1 Variable mass

The upper panel of Fig. 2 shows the growth times of the unstable modes for each of the chosen stellar-mass models for $f = -2$ and

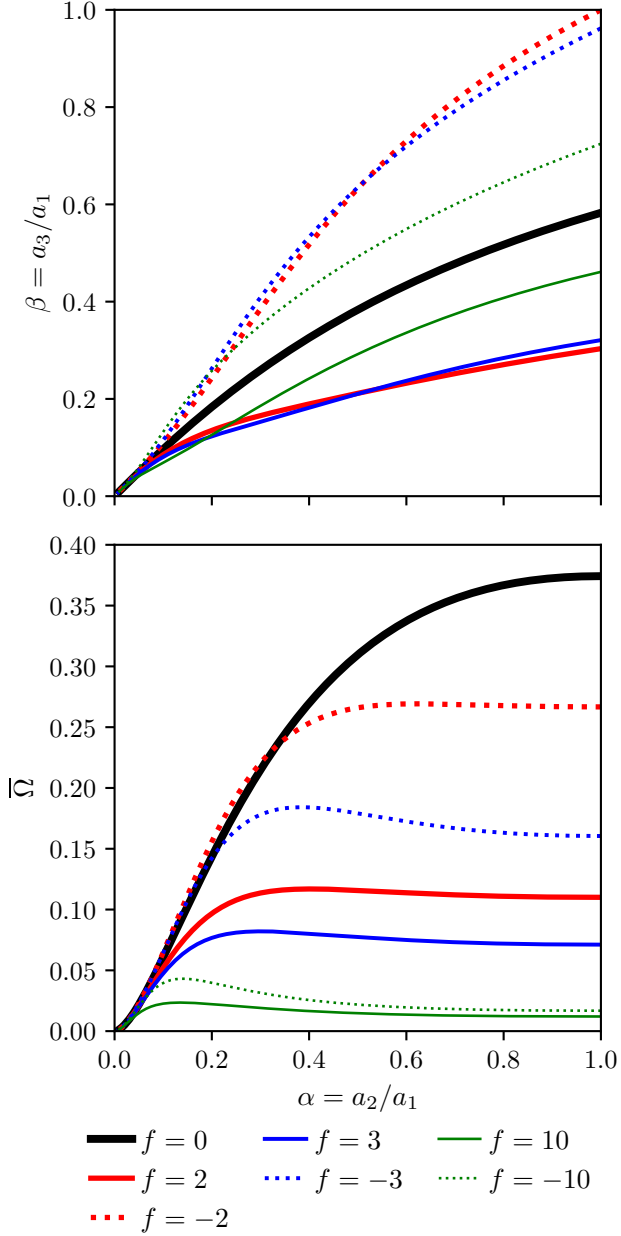


Figure 1. Equilibrium sequences of Riemann S-ellipsoids parametrized by the reduced values of the semi-major axes $\alpha = a_2/a_1$ and $\beta = a_3/a_1$ for several values of circulation parameter f (upper panel). The corresponding non-dimensional rotation frequency $\bar{\Omega}$ is shown in the lower panel. Note that $f = -2$ corresponds to the irrotational case and $f = 0$ to the rigidly rotating case. In the limit $f \rightarrow \pm\infty$ the rotation frequency $\bar{\Omega} \rightarrow 0$.

M/M_\odot	ρ/ρ_0
2	2.64
2.5	3.30
2.75	3.64
3	3.96
3.25	4.29
3.5	4.62

Table 1. The six stellar models studied, listing their masses and densities (in units of the nuclear saturation density $\rho_0 = 2.7 \times 10^{14}$ g/cm³).

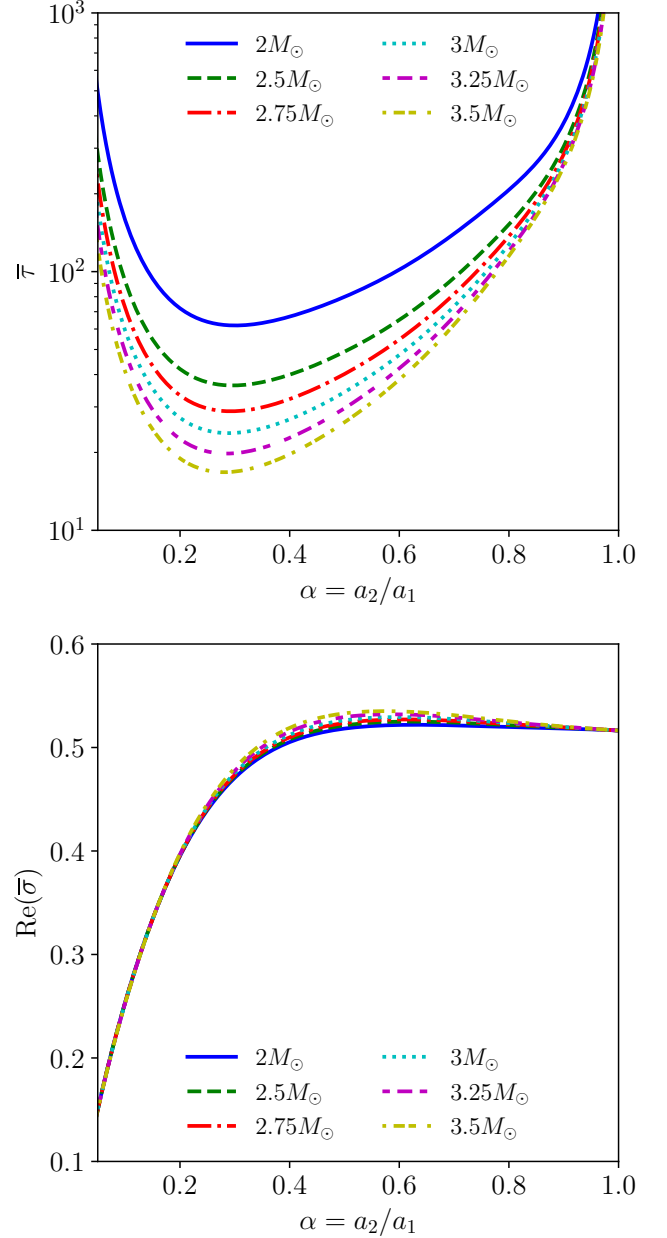


Figure 2. Growth time of unstable (odd) modes τ_o in reduced units for variable mass, $f = -2$, and $\nu = 10^{14}$ cm²/s (upper panel) and the corresponding oscillation frequencies $\text{Re}(\bar{\sigma}_o)$ (lower panel).

with fixed viscosity $\nu = 10^{14}$ cm²/s. The oscillation frequencies corresponding to these unstable modes are shown in the lower panel of the same figure. Note the absence of the instability for the even modes for $f = -2$, which is true generally for $f < 0$. Also note that the oscillation frequencies are almost independent of the mass, which is consistent with our restriction to studying the perturbative modes with $\text{Re}(\sigma_0) \gg |\delta\sigma|$, where σ_0 corresponds to the non-dissipative limit. Figure 3 is identical to the previous figure except now $f = 2$. The minimum growth times for the $f = 2$ unstable modes occur at $\alpha \approx 0.25$, and correspond to numerical values (restoring dimensionality) of 1.1–4.9 ms. For $f = 2$, the minimum growth times for the unstable even and odd modes are similar, with the minimum occurring at $\alpha \approx 0.18$ for the unstable odd modes and at $\alpha \approx 0.11$ for the unstable even modes. The unstable odd modes are unstable for

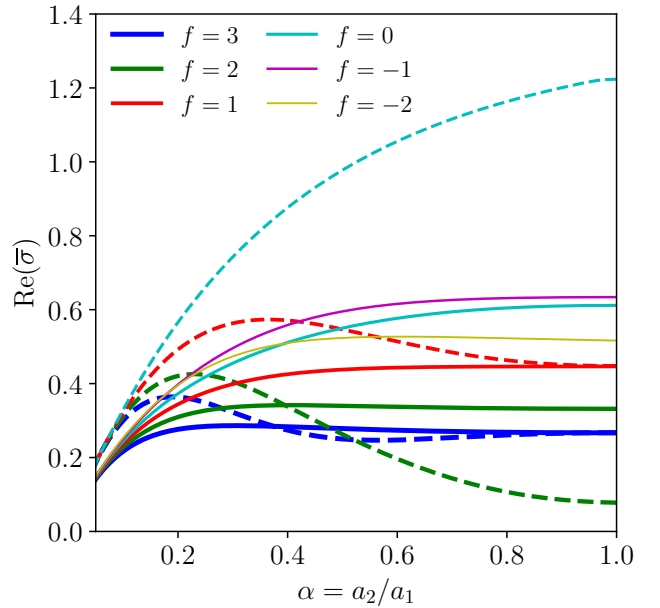
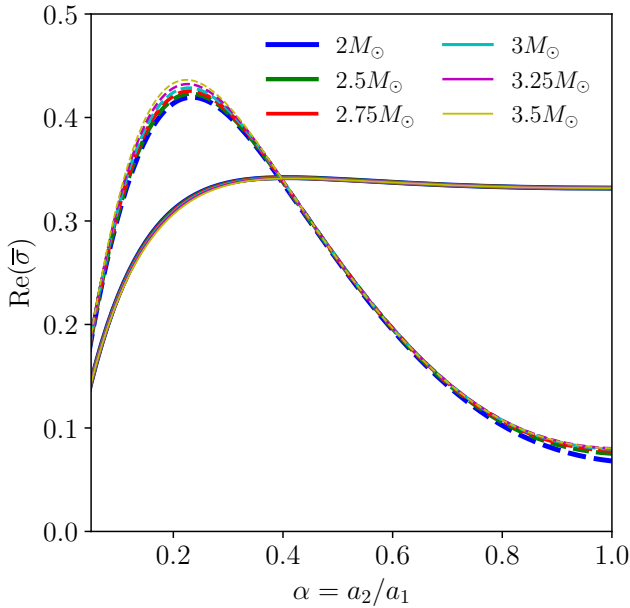
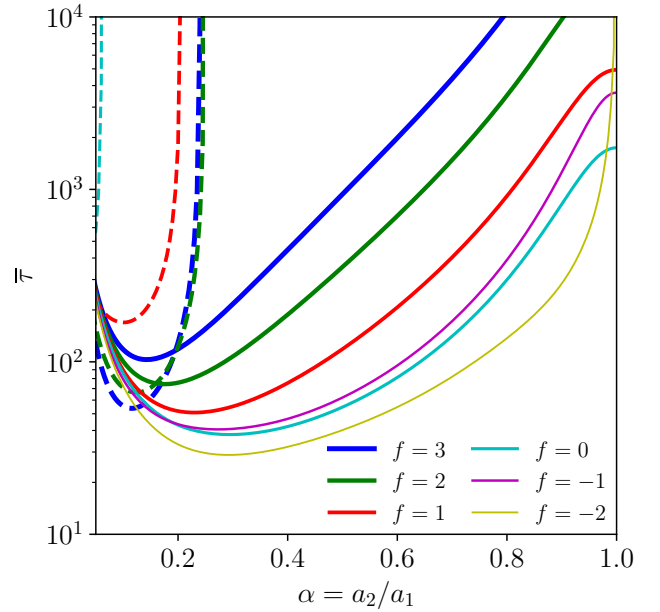
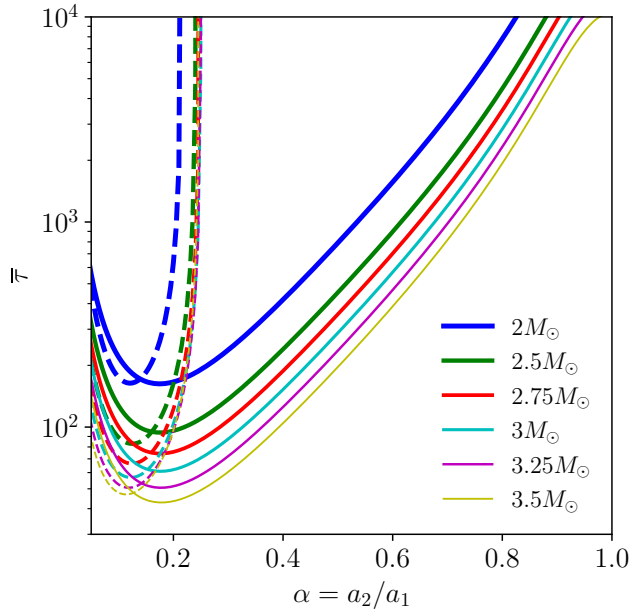


Figure 3. Same as in Fig. 2 except for $f = 2$. In each panel solid lines show the relevant quantities (τ or $\text{Re}(\bar{\sigma})$) for odd modes and dashed lines - for even modes.

Figure 4. Growth time of unstable modes in reduced units for variable f with $M = 2.75M_{\odot}$ and $\nu = 10^{14} \text{ cm}^2/\text{s}$ (upper panel) and the corresponding oscillation frequencies $\text{Re}(\bar{\sigma})$ (lower panel). Solid lines represent τ_o or $\text{Re}(\bar{\sigma}_o)$; dashed lines τ_e or $\text{Re}(\bar{\sigma}_e)$.

all α , with the growth time increasing as $\alpha \rightarrow 1$. In the $f = -2$ case, τ_o approaches infinity as $\alpha \rightarrow 1$ since the $f = -2$ ellipsoid does not have a mass quadrupole moment when $\alpha = \beta = 1$. Changing the mass has a very modest effect on the oscillation frequencies as expected from our imposed restriction to the perturbative modes with $\text{Re}(\sigma) \approx \text{Re}(\sigma_0)$, since the modes of the undamped star (computed in EFE) are independent of the stellar density and hence should only be slightly modified by the gravitational radiation back-reaction.

Figures 4 and 5 show in the upper panels the growth times of the unstable modes for the $M = 2.75M_{\odot}$ and $M = 3.5M_{\odot}$ stellar models for varying f . The even modes for $f < 0$ are not unstable, though the instability in the $f = 0$ case is of little physical interest since it only occurs for unreasonably eccentric ellipsoids. The instability of the even modes only occurs for highly eccentric ellipsoids $\alpha \lesssim 0.25$,

and their minimum growth times are shorter than the growth times for the unstable odd mode for the same stellar model for $f \geq 2$. The corresponding oscillation frequencies are shown in the lower panel of Figs. 4. For small $\alpha \approx 0.1$ the mode frequencies converge to the same value with distinct but similar values for odd and even modes. As α increases the odd modes saturate at a constant value starting from $\alpha \gtrsim 0.3-0.4$. The frequencies of the even modes pass through a maximum and decay for large α except for $f = 0$ case which increases monotonically up to the point $\alpha = 1$.

The GW-unstable odd modes occur for all equilibrium ellipsoids except the perfectly spherical $f = -2$, $\alpha = 1$ model, unlike the even unstable modes which only appear for highly eccentric ellipsoids. When the viscosity is lowered, the instability for the less-eccentric

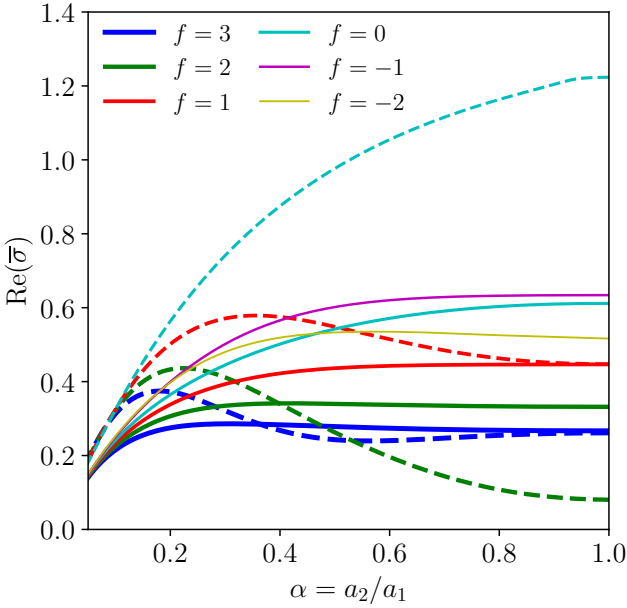
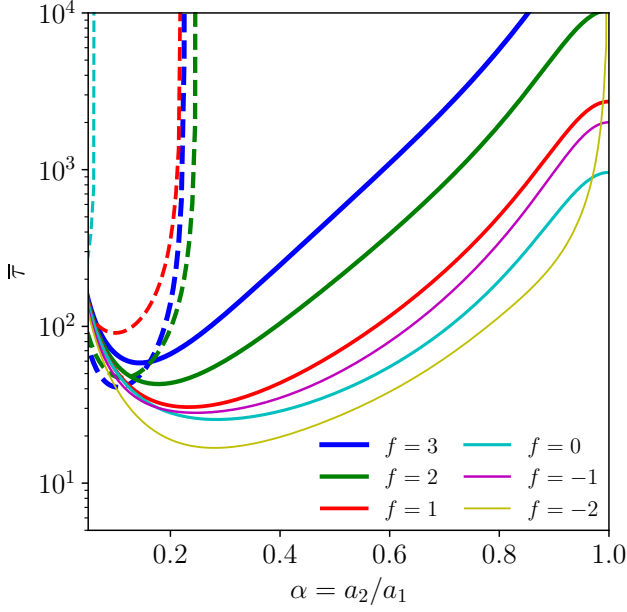


Figure 5. Same as Fig. 4 except for $M = 3.5M_{\odot}$.

ellipsoids can occur, as is shown in the next section. The presence or absence of this instability could hint at the sizes of the viscosities present in HMNS.

3.2 Variable viscosity

As discussed in our previous work (Rau & Sedrakian 2020), exaggerated viscosities compared to those that have been computed for neutron star interiors using usual transport theory [for a review see (Schmitt & Shternin 2018)] are required for the viscosity to have any effect on the modes. The required kinematic viscosities for physical relevance are of order 10^{12} – 10^{14} $\text{cm}^2 \text{s}^{-1}$, which are far above the typical values of $\nu \sim 10$ – 10^3 $\text{cm}^2 \text{s}^{-1}$ for a neutron star core, assuming that the matter in the HMNS is similar to a neutron star but at higher temperatures $T \sim 10^{10}$ – 10^{12} K. However, they are consistent

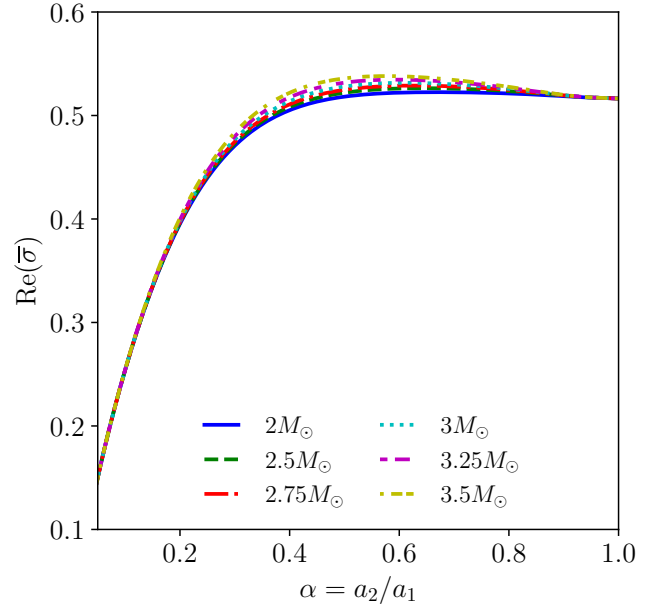
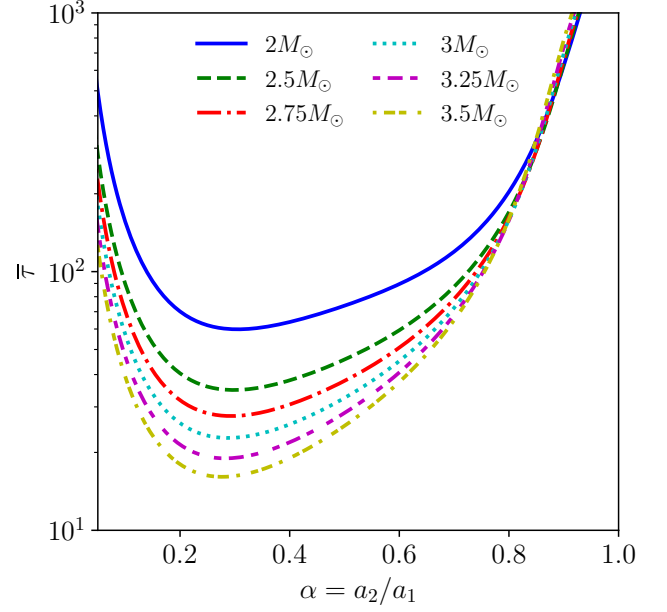


Figure 6. The growth times as in Fig. 2 except with $\nu = 10^{13} \text{ cm}^2 \text{ s}^{-1}$ (upper panel) and the corresponding oscillation frequencies $\text{Re}(\bar{\omega})$ (lower panel).

with typical turbulent viscosities used in astrophysical applications, including binary neutron star merger simulations (Fujibayashi et al. 2018). This is most often implemented using the Shakura–Sunyaev α -parameter prescription (Shakura & Sunyaev 1973)

$$\nu = \alpha_{\text{visc}} c_s H_{\text{turb}}, \quad (37)$$

where α_{visc} is the dimensionless α -parameter, $c_s \sim c/3$ is the sound speed and $H_{\text{turb}} \sim 10^6$ cm is the turbulent eddy scale height, which should be of order the radius of the star. The range of nonzero viscosities we consider, $\nu = 5 \times 10^{12}$ – 10^{14} cm^2/s , are thus consistent with $\alpha_{\text{visc}} \sim 0.0005$ – 0.01 .

Figures 6 and 7 show in the upper panels the growth times of the unstable modes for each of the chosen stellar-mass models for $f = -2$ and $f = 2$ respectively, with fixed viscosity $\nu = 10^{13}$ cm^2/s . The corresponding oscillation frequencies are shown in the lower

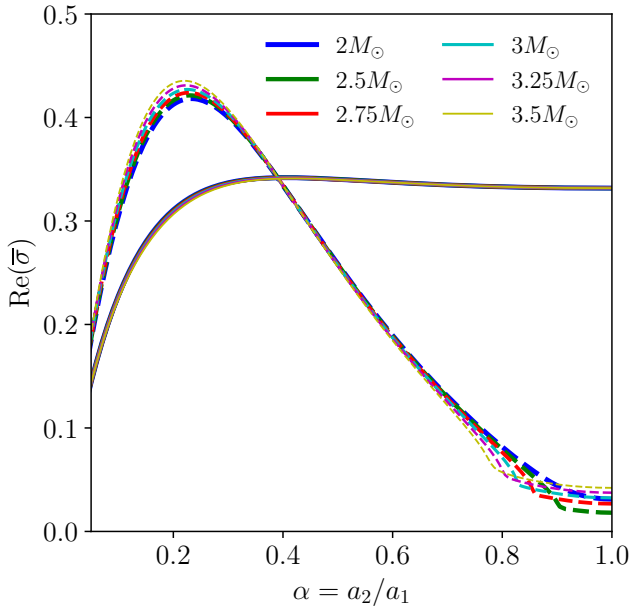
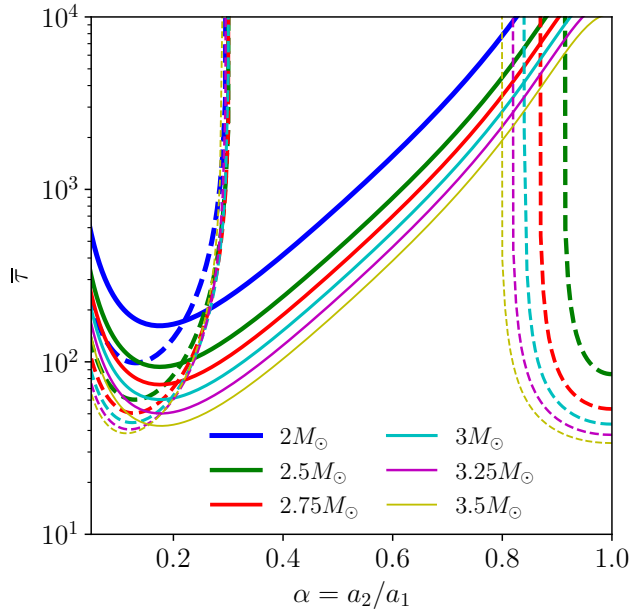


Figure 7. The growth times as in Fig. 3 except with $\nu = 10^{13} \text{ cm}^2 \text{ s}^{-1}$. (upper panel) and the corresponding oscillation frequencies $\text{Re}(\bar{\sigma})$ (lower panel).

panels, respectively. Comparing to Figs. 2 and 3, we see that the growth times for the more eccentric ellipsoids $\alpha \lesssim 0.4$ are nearly unaffected by the change in viscosity. This is to be expected since the quadrupole moment of the ellipsoid increases with eccentricity and the gravitational radiation thus dominates the viscosity. Most notably, lowering the viscosity opens up a second “branch” of instability for the unstable even modes for $f > 0$: they are also unstable at large $\alpha \gtrsim 0.8$ in addition to at $\alpha \lesssim 0.25$, with comparable minimum growth times for both branches. However, at $\nu = 10^{13} \text{ cm}^2/\text{s}$, the instability for $\alpha \gtrsim 0.8$ is suppressed in the $2M_\odot$ ellipsoid: lowering the viscosity further allows this ellipsoid to be unstable in this range of α as shown later.

Figure 8–11 show the growth times and oscillation frequencies of the $f = 2$ unstable modes for varying ν and $M = 2M_\odot, 2.5M_\odot, 3M_\odot$

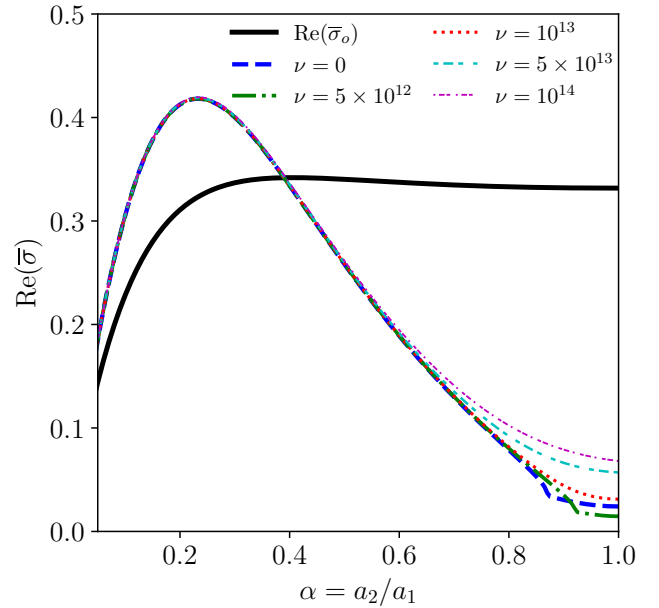
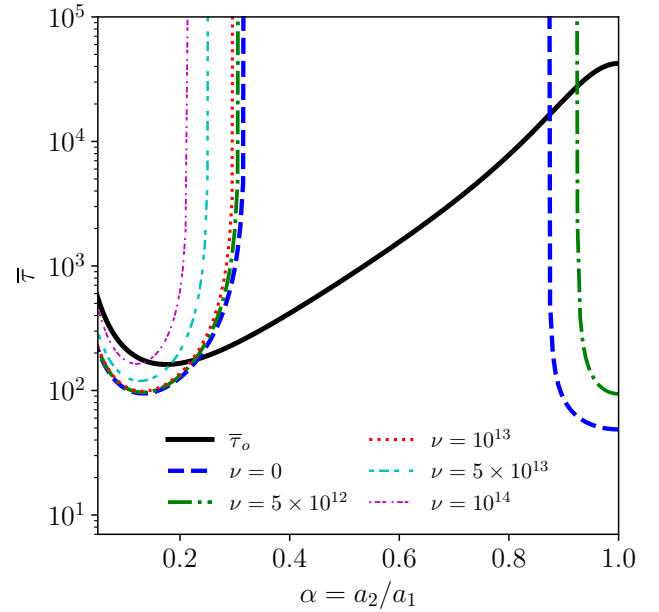


Figure 8. Growth time of unstable modes in reduced units for variable ν with $M = 2M_\odot$ and $f = 2$ (upper panel) and the corresponding oscillation frequencies $\text{Re}(\bar{\sigma})$ (lower panel). The growth time of the unstable odd mode is not modified by changing the viscosity, and the τ_e and $\text{Re}(\sigma_e)$ are shown as non-solid lines. The viscosities are given in units of $\text{cm}^2 \text{ s}^{-1}$.

and $3.5M_\odot$ stellar models respectively. The gravitational-radiation-unstable odd modes are unchanged by varying the viscosity for fixed f and stellar mass. This is why only a single value of τ_o is included in each figure. In general, increasing the viscosity increases the growth times i.e. has a stabilizing effect as expected. Note that for the $M = 2.5M_\odot, 3M_\odot$ and $3.5M_\odot$ models, the high α branch of the instability vanishes above $\nu = 10^{13} \text{ cm}^2/\text{s}$, while for the $M = 2M_\odot$ model it vanishes above $\nu = 5 \times 10^{12} \text{ cm}^2/\text{s}$. For $\alpha \lesssim 0.75$, the values of $\text{Re}(\sigma_e)$ for the different choices of ν are equal to within a few percent, as expected for analogous reasons as to why $\text{Re}(\sigma)$ is only slightly changed as a function of mass for fixed f . For larger values

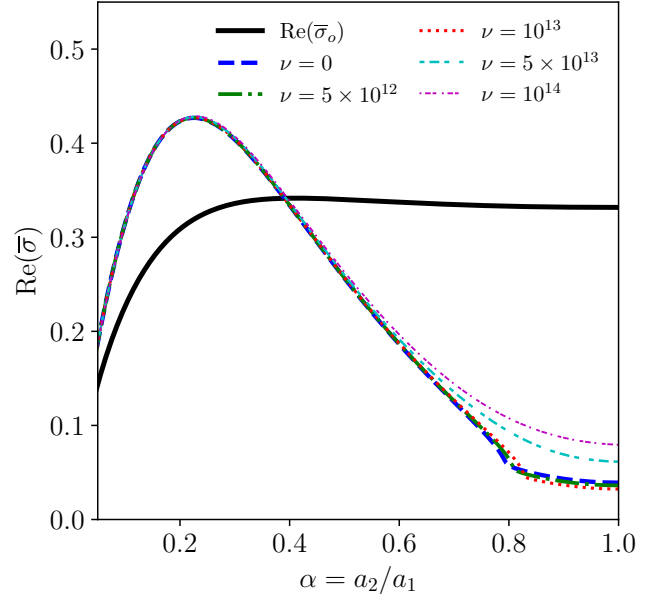
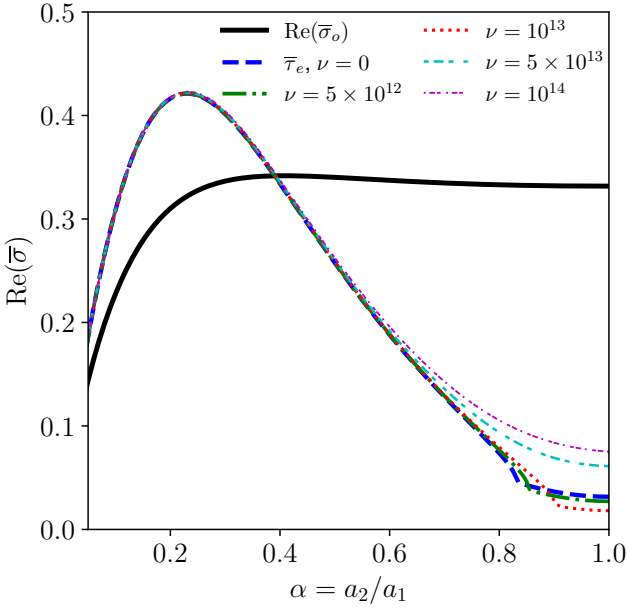
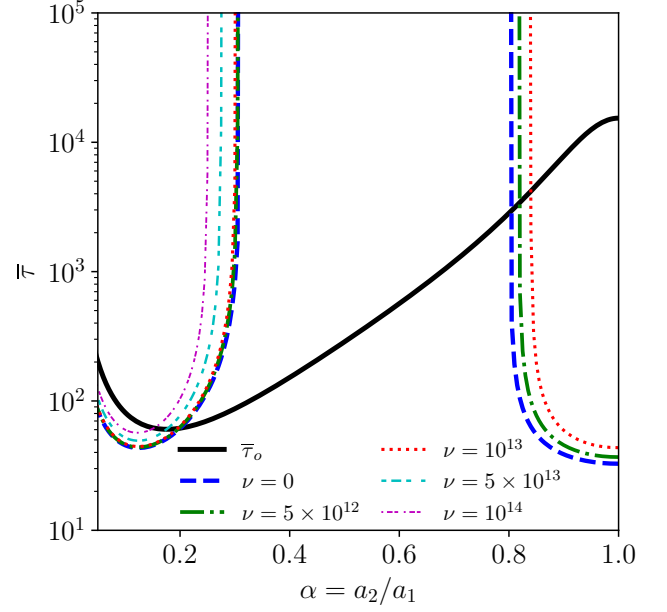
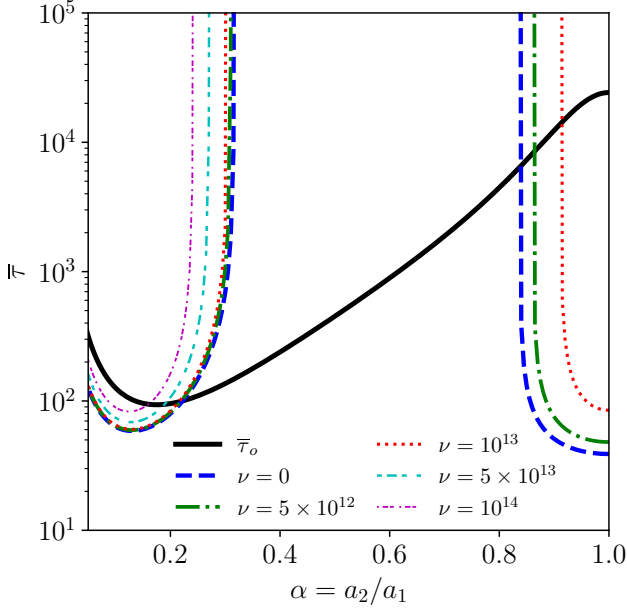


Figure 9. Same as Fig. 8 except with $M = 2.5M_\odot$.

Figure 10. Same as Fig. 8 except with $M = 3M_\odot$.

of α there can be a significant difference in $\text{Re}(\sigma_e)$ as a function of viscosity

4 CONCLUSION

In this paper, we have provided further details on the gravitational-radiation-unstable modes of Riemann S-type ellipsoids as computed using the tensor-virial method, and made comparisons of the unstable modes for different masses and viscosities. The range of masses examined are appropriate for simple models of transient, rapidly-rotating hypermassive neutron stars formed in BNS mergers. The calculations here and in [Rau & Sedrakian \(2020\)](#) give qualitative estimates for the growth times and oscillation frequencies of the unstable modes of HMNS, assuming they can settle into quasi-stationary grav-

itational equilibria shortly after their birth and before the collapse to a black hole.

As expected, the growth times of the unstable modes generally increase as a function of the stellar mass. They are of order milliseconds, i.e., short enough to be relevant to HMNS. The growth times are increased by viscosity, and its magnitude should be of order $\nu \approx 10^{12}$ cm^2/s or larger to have an observable effect on the unstable growth times for the range of masses we considered. These values are impossible with only standard viscosities computed using transport theory (e.g. using the Chapman–Enskog expansion), but are attainable via turbulent viscosity as applied in accretion disk theory and in numerical BNS merger simulations. For $\nu \gtrsim 10^{15}$ cm^2/s , the instability can be suppressed completely. In general, the even unstable modes, corresponding to toroidal perturbations, have slightly longer growth times for a given f , mass and viscosity than the transverse-shear perturbation odd modes. The even modes are unstable for highly ec-

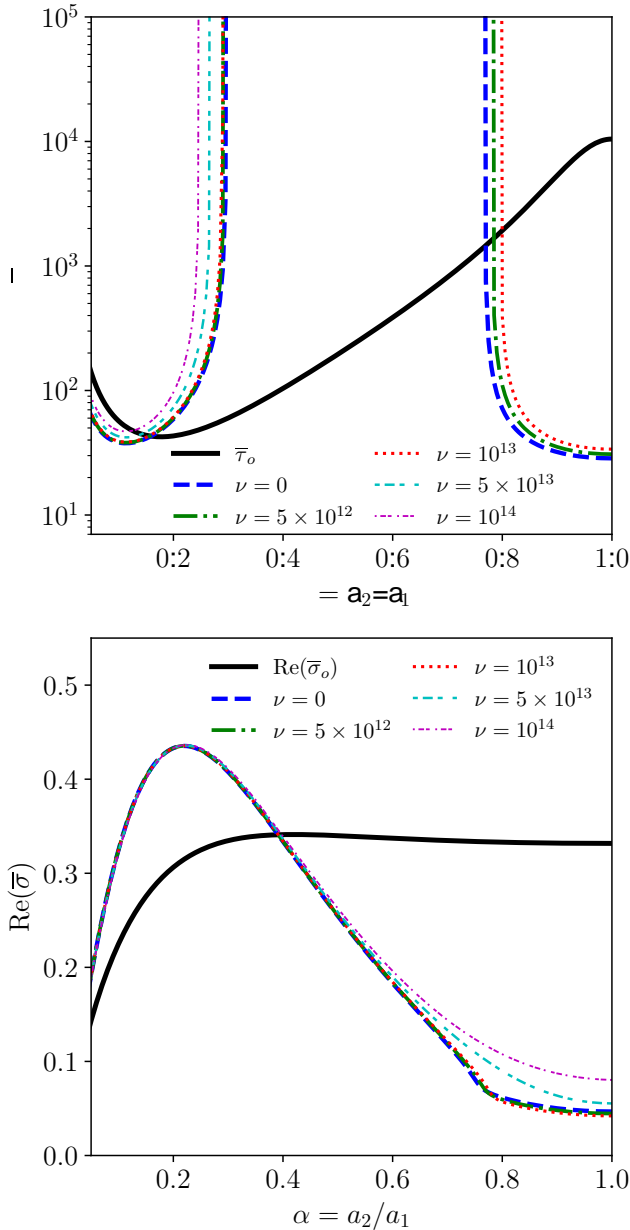


Figure 11. Same as FIG. 8 except with $M = 3.5M_\odot$.

centric ellipsoids $\alpha = a_3/a_1 \lesssim 0.25$ for $f \geq 0$, and can be unstable for $\alpha \gtrsim 0.8$ and $f \geq 0$ if the viscosity is sufficiently small. The odd modes are unstable for all α except the spherical $\alpha = 1$, $f = -2$ stellar model, and have growth times that are minimized near $\alpha \approx 0.25$.

The insights gained here from the semi-analytical tensor-virial approach are expected to be useful when addressing the problem of HMNS oscillations in different settings and approximations, in particular when including such features as realistic equations of state, general relativity, and varying velocity profiles (with slowly rotating core and rapidly rotating envelope) as seen in the numerical simulations of BNS mergers. We anticipate that the instabilities of the oscillation modes revealed in our analysis will be present in more realistic models, as has been the case for self-gravitating fluids without internal circulations.

It is worthwhile to note that the oscillations of the type discussed here can be tested in the laboratory using ultracold atoms, for which

the magnetic or laser trapping potential takes the role of the gravitational potential. For such systems, the tensor-virial method leads to a good agreement between the theory and experiment, as has been demonstrated in the case of the breathing modes of uniformly rotating clouds (Sedrakian & Wasserman 2001; Watanabe 2007).

5 ACKNOWLEDGEMENTS

We are grateful to I. Wasserman for discussions. AS acknowledges the support by the Deutsche Forschungsgemeinschaft (Grant No. SE 1836/5-1) and the European COST Action CA16214 PHAROS ‘‘The multi-messenger physics and astrophysics of neutron stars’’.

DATA AVAILABILITY

The data underlying this article will be shared on reasonable request to the corresponding author.

REFERENCES

- Andersson N., 2021, *Universe*, 7, 1
- Bauswein A., Stergioulas N., Janka H. T., 2014, *Phys. Rev. D*, 90, 1
- Bauswein A., Just O., Janka H. T., Stergioulas N., 2017, *Astrophys. J. Lett.*, 850, L34
- Chandrasekhar S., 1969, *Ellipsoidal Figures of Equilibrium*. Yale University Press, New Haven
- Chandrasekhar S., 1970, *Astrophys. J.*, 161, 561
- Chandrasekhar S., Elbert D., 1974, *Astrophys. J.*, 192, 731
- Chandrasekhar S., Esposito F. P., 1970, *Astrophys. J.*, 160, 153
- Chaurasia S. V., Dietrich T., Ujevic M., Hendriks K., Dudi R., Fabbri F. M., Tichy W., Brügmann B., 2020, *Phys. Rev. D*, 102, 024087
- Cromartie H. T., et al., 2020, *Nat. Astron.*, 4, 72
- Detweiler S. L., Lindblom L., 1977, *Astrophys. J.*, 213, 193
- Dietrich T., Bernuzzi S., Ujevic M., Tichy W., 2017, *Phys. Rev. D*, 95, 044045
- Friedman J. L., Schutz B. F., 1978, *Astrophys. J.*, 221, 937
- Fujibayashi S., Kiuchi K., Nishimura N., Sekiguchi Y., Shibata M., 2018, *Astrophys. J.*, 860, 64
- Gill R., Nathanael A., Rezzolla L., 2019, *Astrophys. J.*, 876, 139
- Gürlebeck N., Petroff D., 2010, *Astrophys. J.*, 722, 1207
- Gürlebeck N., Petroff D., 2013, *Astrophys. J.*, 777
- Hanuske M., et al., 2019, *Particles*, 2, 44
- Kastaun W., Galeazzi F., 2015, *Phys. Rev. D*, 91, 062027
- Kastaun W., Cioffi R., Endrizzi A., Giacomazzo B., 2017, *Phys. Rev. D*, 96, 043019
- Kokkotas K. D., Schwenzer K., 2016, *Eur. Phys. J. A*, 52, 1
- LIGO Scientific Collaboration and Virgo Collaboration: et al., 2017, *Phys. Rev. Lett.*, 119, 161101
- LIGO Scientific Collaboration and Virgo Collaboration: et al., 2019, *Astrophys. J.*, 875, 160
- LIGO Scientific Collaboration and Virgo Collaboration: et al., 2021, *Phys. Rev. X*, 11, 021053
- Lai D., Shapiro S. L., 1995, *Astrophys. J.*, 442, 259
- Lai D., Rasio F. A., Shapiro S., 1993, *Astrophys. J. Suppl. Ser.*, 88, 205
- Lai D., Rasio F. A., Shapiro S. L., 1994, *Astrophys. J.*, 437, 742
- Maggiore M., et al., 2020, *J. Cosmology Astropart. Phys.*, 2020, 050
- Margalit B., Metzger B. D., 2017, *Astrophys. J.*, 850, L19
- Miller B. D., 1974, *Astrophys. J.*, 609-620, 609
- Misner C. W., Thorne K. S., Wheeler J. A., 1973, *Gravitation*. W. H. Freeman, San Francisco
- Most E. R., Jens Papenfort L., Rezzolla L., 2019, *Mon. Not. R. Astron. Soc.*, 490, 3588
- Press W. H., Teukolsky S. A., 1973, *Astrophys. J.*, 181, 513
- Radice D., Perego A., Bernuzzi S., Zhang B., 2018, *Mon. Not. R. Astron. Soc.*, 481, 3670

- Rau P. B., Sedrakian A., 2020, *Astrophys. J. Lett.*, 902, L41
 Reitze D., et al., 2019, in *Bulletin of the American Astronomical Society*.
 p. 35 ([arXiv:1907.04833](https://arxiv.org/abs/1907.04833))
 Roberts P. H., Stewartson K., 1963, *Astrophys. J.*, 137, 777
 Rosenkilde C. E., 1967, *Astrophys. J.*, 148, 825
 Ruiz M., Tsokaros A., Shapiro S. L., 2020, *Phys. Rev. D*, 101, 064042
 Schmitt A., Shternin P., 2018, in Rezzolla L., Pizzochero P., Jones D. I.,
 Rea N., Vidiña I., eds., *The Physics and Astrophysics of Neutron Stars*.
 Springer, Heidelberg, Chapt. 9, pp 455–574
 Sedrakian A., Wasserman I., 2001, *Phys. Rev. D*, 63, 024016
 Shakura N. I., Sunyaev R. A., 1973, *Astron. Astrophys.*, 24, 337
 Shapiro S. L., Zane S., 1998, *Astrophys. J. Suppl. Ser.*, 117, 531
 Shibata M., Fujibayashi S., Hotokezaka K., Kiuchi K., Kyutoku K., Sekiguchi
 Y., Tanaka M., 2017, *Phys. Rev. D*, 96, 123012
 Stergioulas N., Bauswein A., Zagkouris K., Janka H. T., 2011, *Mon. Not. R.*
Astron. Soc., 418, 427
 Takami K., Rezzolla L., Baiotti L., 2014, *Phys. Rev. Lett.*, 113, 1
 Thorne K. S., 1969, *Astrophys. J.*, 158, 997
 Watanabe G., 2007, *Phys. Rev. A*, 76, 031601
 Weih L. R., Most E. R., Rezzolla L., 2018, *Mon. Not. R. Astron. Soc.*, 473,
 L126

APPENDIX A: GRAVITATIONAL RADIATION BACK-REACTION TERM IN VIRIAL EQUATION 1: LOWEST ORDER FORM

The gravitational radiation back-reaction potential Φ_{GW} in the weak-
 field, slow motion regime is (Misner et al. 1973; Lai et al. 1994)

$$\Phi_{\text{react}} = -\frac{G}{5c^5} \mathcal{I}_{ij}^{(5)} x_i x_j. \quad (\text{A1})$$

The corresponding gravitational radiation back-reaction force is
 given by (Miller 1974)

$$\begin{aligned} f_i^{\text{react}} &= -\rho \frac{\partial \Phi_{\text{react}}}{\partial x^k} = \frac{2\rho G}{5c^2} \left(\mathcal{I}_{ik}^{(5)} x_k - \frac{1}{3} \mathcal{I}_{kk}^{(5)} x_i \right) \\ &= \frac{2\rho G}{5c^2} \mathcal{I}_{ik}^{(5)} x_k, \end{aligned} \quad (\text{A2})$$

which leads to the second moment of this expression

$$\mathcal{G}_{ij} = \frac{2G}{5c^5} \int_{\mathcal{V}} d^3x \rho \mathcal{I}_{ik}^{(5)} x_k x_j. \quad (\text{A3})$$

Taking the perturbation of this tensor we find

$$\begin{aligned} \delta \mathcal{G}_{ij} &= \frac{2G}{5c^5} \left(\mathcal{I}_{ik}^{(5)} V_{kj} + \int_{\mathcal{V}} d^3x \rho x_k x_j \delta \mathcal{I}_{ik}^{(5)} \right) \\ &= \frac{2G}{5c^5} \left(\mathcal{I}_{ik}^{(5)} V_{kj} + \mathcal{V}_{ik}^{(5)} I_{kj} \right), \end{aligned} \quad (\text{A4})$$

where

$$\delta I_{ij} = \delta \int_{\mathcal{V}} d^3x \rho x_i x_j = V_{ij}. \quad (\text{A5})$$

and, since $\delta I_{ij} = \delta I_{ij}^{(r)}$ in a rotating frame,

$$\begin{aligned} \delta I_{ij}^{(5)} &= \sum_{m=0}^5 \sum_{p=0}^m C_m^5 C_p^m (-1)^p \\ &\quad \times [(\bar{\mathbf{\Omega}}^*)^p]_{ik} \frac{d^{5-m} \delta I_{k\ell}^{(r)}}{dt^{5-m}} [(\bar{\mathbf{\Omega}}^*)^{m-p}]_{\ell j} \\ &\equiv V_{ij}^{(5)}. \end{aligned} \quad (\text{A6})$$

Eq. (A4) includes the secular effects of gravitational radiation back-
 reaction for quadrupole radiation (Thorne 1969). Additional effects
 at higher orders in a post-Newtonian expansion can be incorporated
 using the formalism of Chandrasekhar & Esposito (1970). As we do
 not include the post-Newtonian effects on the background ellipsoid
 and in the tensor-virial formalism, it would be inconsistent to use
 these more-complicated gravitational radiation back-reaction terms
 in this paper.

APPENDIX B: CHARACTERISTIC EQUATIONS

We explicitly write the nine different components of Eq. (2) in terms of the V_{ij} and $V_{i;j}$, the rotation frequency Ω and ratio f , the eigenvalue λ , the index symbols B_{ij} and A_{ij} , and the mass and principal axes of the equilibrium ellipsoids. The five components even in the index 3 are

$$\frac{1}{2}\lambda^2 V_{33} = -\pi G\rho \left[2B_{33}V_{33} - a_3^2 \sum_{\ell=1}^3 A_{3\ell}V_{\ell\ell} \right] - \frac{5\lambda\eta}{a_3^2} V_{33} - \frac{2GM(a_1^2 + a_2^2)}{75c^5} \lambda^5 (2V_{33} - V_{11} - V_{22}) + \delta\Pi, \quad (\text{B1})$$

$$\begin{aligned} \left[\frac{1}{2}\lambda^2 + Q_{12}Q_{21} - \Omega^2 \right] V_{11} - 2\lambda Q_{12}V_{1;2} - 2\lambda\Omega V_{2;1} - \Omega(Q_{21}V_{11} - Q_{12}V_{22}) = & -\pi G\rho \left[2B_{11}V_{11} - a_1^2 \sum_{\ell=1}^3 A_{1\ell}V_{\ell\ell} \right] + \delta\Pi \\ & - 5\eta \left[\frac{\lambda V_{11}}{a_1^2} + 2Q_{21} \frac{V_{1;2}}{a_2^2} - 2Q_{12} \frac{V_{2;1}}{a_1^2} \right] \\ - \frac{2GM(a_2^2 + a_3^2)}{25c^5} \left[\frac{1}{3}\lambda^5 (2V_{11} - V_{22} - V_{33}) - \phi_1(\lambda, \Omega)(V_{11} - V_{22}) + \left(16\Omega^5 \frac{a_2^2 - a_1^2}{a_2^2 + a_3^2} - 2\phi_2(\lambda, \Omega) \right) V_{12} \right], & (\text{B2}) \end{aligned}$$

$$\begin{aligned} \left[\frac{1}{2}\lambda^2 + Q_{12}Q_{21} - \Omega^2 \right] V_{22} - 2\lambda Q_{21}V_{2;1} + 2\lambda\Omega V_{1;2} + \Omega(Q_{12}V_{22} - Q_{21}V_{11}) = & -\pi G\rho \left[2B_{22}V_{22} - a_2^2 \sum_{\ell=1}^3 A_{2\ell}V_{\ell\ell} \right] + \delta\Pi \\ & - 5\eta \left[\frac{\lambda V_{22}}{a_2^2} + 2Q_{12} \frac{V_{2;1}}{a_1^2} - 2Q_{21} \frac{V_{1;2}}{a_2^2} \right] \\ - \frac{2GM(a_1^2 + a_3^2)}{25c^5} \left[\frac{1}{3}\lambda^5 (2V_{22} - V_{11} - V_{33}) - \phi_1(\lambda, \Omega)(V_{22} - V_{11}) + \left(16\Omega^5 \frac{a_2^2 - a_1^2}{a_1^2 + a_3^2} + 2\phi_2(\lambda, \Omega) \right) V_{12} \right], & (\text{B3}) \end{aligned}$$

$$\begin{aligned} \lambda^2 V_{1;2} - \lambda Q_{21}V_{11} - \lambda\Omega V_{22} = & -5\eta \left[\lambda \left(\frac{V_{1;2}}{a_2^2} + \frac{V_{2;1}}{a_1^2} \right) + \frac{Q_{12} - Q_{21}}{2} \left(\frac{V_{11}}{a_1^2} - \frac{V_{22}}{a_2^2} \right) \right] \\ - \frac{2GM(a_1^2 + a_3^2)}{25c^5} \left[16\Omega^5 \frac{a_2^2 - a_1^2}{a_1^2 + a_3^2} V_{22} + (\lambda^5 - 2\phi_1(\lambda, \Omega))V_{12} + \phi_2(\lambda, \Omega)(V_{11} - V_{22}) \right], & (\text{B4}) \end{aligned}$$

$$\begin{aligned} \lambda^2 V_{2;1} - \lambda Q_{12}V_{22} + \lambda\Omega V_{11} = & -5\eta \left[\lambda \left(\frac{V_{1;2}}{a_2^2} + \frac{V_{2;1}}{a_1^2} \right) + \frac{Q_{12} - Q_{21}}{2} \left(\frac{V_{11}}{a_1^2} - \frac{V_{22}}{a_2^2} \right) \right] \\ - \frac{2GM(a_2^2 + a_3^2)}{25c^5} \left[16\Omega^5 \frac{a_2^2 - a_1^2}{a_2^2 + a_3^2} V_{11} + (\lambda^5 - 2\phi_1(\lambda, \Omega))V_{12} + \phi_2(\lambda, \Omega)(V_{11} - V_{22}) \right], & (\text{B5}) \end{aligned}$$

where in the last two equations we used the relation $\Omega^2 - Q_{12}Q_{21} = 2B_{12}$ valid for Riemann ellipsoids with parallel ω and Ω . The four components odd in the index 3 are

$$\begin{aligned} \lambda^2 V_{1;3} - 2\lambda\Omega V_{2;3} + Q_{12}Q_{21}V_{3;1} - 2\Omega Q_{21}V_{3;1} = & (\Omega^2 - 2\pi G\rho B_{13})V_{13} - 5\lambda\eta \left(\frac{V_{1;3}}{a_3^2} + \frac{V_{3;1}}{a_1^2} \right) \\ & - \frac{2GM(a_1^2 + a_2^2)}{25c^5} \lambda^5 V_{13} - \frac{32GM(a_2^2 - a_1^2)}{25c^5} \Omega^5 V_{23}, & (\text{B6}) \end{aligned}$$

$$\begin{aligned} \lambda^2 V_{2;3} + 2\lambda\Omega V_{1;3} + Q_{12}Q_{21}V_{3;2} + 2\Omega Q_{12}V_{3;2} = & (\Omega^2 - 2\pi G\rho B_{23})V_{23} - 5\eta \left(\lambda \frac{V_{2;3}}{a_3^2} + \lambda \frac{V_{3;2}}{a_2^2} + Q_{12} \frac{V_{3;1}}{a_1^2} - Q_{21} \frac{V_{1;3}}{a_3^2} \right) \\ & - \frac{2GM(a_1^2 + a_2^2)}{25c^5} \lambda^5 V_{23} - \frac{32GM(a_2^2 - a_1^2)}{25c^5} \Omega^5 V_{13}, & (\text{B7}) \end{aligned}$$

$$\begin{aligned} \lambda^2 V_{3;1} - 2\lambda Q_{12}V_{3;2} + Q_{12}Q_{21}V_{3;1} = & -2\pi G\rho B_{13}V_{13} - 5\lambda\eta \left(\frac{V_{3;1}}{a_1^2} + \frac{V_{1;3}}{a_3^2} \right) \\ & - \frac{2GM(a_2^2 + a_3^2)}{25c^5} \left([\lambda^5 - \phi_1(\lambda, \Omega)]V_{13} - \phi_2(\lambda, \Omega)V_{23} \right), & (\text{B8}) \end{aligned}$$

$$\begin{aligned} \lambda^2 V_{3;2} - 2\lambda Q_{21}V_{3;1} + Q_{12}Q_{21}V_{3;2} = & -2\pi G\rho B_{23}V_{23} - 5\eta \left(\lambda \frac{V_{3;2}}{a_2^2} + \lambda \frac{V_{2;3}}{a_3^2} + Q_{12} \frac{V_{3;1}}{a_1^2} - Q_{21} \frac{V_{1;3}}{a_3^2} \right) \\ & - \frac{2GM(a_1^2 + a_3^2)}{25c^5} \left([\lambda^5 - \phi_1(\lambda, \Omega)]V_{23} + \phi_2(\lambda, \Omega)V_{13} \right). & (\text{B9}) \end{aligned}$$

Eqs. (B1)–(B9) can be divided by $\pi G\rho$, which makes all the coefficients of $V_{i;j}$ and V_{ij} dimensionless. The reduced equations are

$$\frac{1}{2}\bar{\lambda}^2 V_{33} = - \left[2\bar{B}_{33} V_{33} - \beta^2 \sum_{\ell=1}^3 \bar{A}_{3\ell} V_{\ell\ell} \right] - \frac{5\bar{\lambda}\bar{\eta}}{\beta^2} V_{33} - \frac{8\alpha\beta(1+\alpha^2)}{225} \bar{t}_c^5 \bar{\lambda}^5 (2V_{33} - V_{11} - V_{22}) + \frac{\delta\Pi}{\pi G\rho}, \quad (\text{B10})$$

$$\left[\frac{1}{2}\bar{\lambda}^2 - \frac{\alpha^2 \bar{\Omega}^2 f^2}{(1+\alpha^2)^2} - \bar{\Omega}^2 \right] V_{11} + \frac{2\bar{\Omega}\bar{\lambda}f}{1+\alpha^2} V_{1;2} - 2\bar{\lambda}\bar{\Omega} V_{2;1} - \frac{\bar{\Omega}^2 f}{1+\alpha^2} (\alpha^2 V_{11} + V_{22}) = - \left[2\bar{B}_{11} V_{11} - \sum_{\ell=1}^3 \bar{A}_{1\ell} V_{\ell\ell} \right] + \frac{\delta\Pi}{\pi G\rho} - 5\bar{\eta} \left[\bar{\lambda} V_{11} + \frac{2\bar{\Omega}f}{1+\alpha^2} V_{12} \right] - \frac{8\alpha\beta(\alpha^2 + \beta^2)}{75} \bar{t}_c^5 \left[\frac{1}{3}\bar{\lambda}^5 (2V_{11} - V_{22} - V_{33}) - \phi_1(\bar{\lambda}, \bar{\Omega})(V_{11} - V_{22}) + \left(16\bar{\Omega}^5 \frac{\alpha^2 - 1}{\alpha^2 + \beta^2} - 2\phi_2(\bar{\lambda}, \bar{\Omega}) \right) V_{12} \right], \quad (\text{B11})$$

$$\left[\frac{1}{2}\bar{\lambda}^2 - \frac{\alpha^2 \bar{\Omega}^2 f^2}{(1+\alpha^2)^2} - \bar{\Omega}^2 \right] V_{22} - \frac{2\alpha^2 \bar{\Omega}\bar{\lambda}f}{1+\alpha^2} V_{2;1} + 2\bar{\lambda}\bar{\Omega} V_{1;2} - \frac{\bar{\Omega}^2 f}{1+\alpha^2} (V_{22} + \alpha^2 V_{11}) = - \left[2\bar{B}_{22} V_{22} - \alpha^2 \sum_{\ell=1}^3 \bar{A}_{2\ell} V_{\ell\ell} \right] + \frac{\delta\Pi}{\pi G\rho} - 5\bar{\eta} \left[\bar{\lambda} \frac{V_{22}}{\alpha^2} - \frac{2\bar{\Omega}f}{1+\alpha^2} V_{12} \right] - \frac{8\alpha\beta(1+\beta^2)}{75} \bar{t}_c^5 \left[\frac{1}{3}\bar{\lambda}^5 (2V_{22} - V_{11} - V_{33}) - \phi_1(\bar{\lambda}, \bar{\Omega})(V_{22} - V_{11}) + \left(16\bar{\Omega}^5 \frac{\alpha^2 - 1}{1+\beta^2} + 2\phi_2(\bar{\lambda}, \bar{\Omega}) \right) V_{12} \right], \quad (\text{B12})$$

$$\bar{\lambda}^2 V_{1;2} - \frac{\alpha^2 \bar{\Omega}\bar{\lambda}f}{1+\alpha^2} V_{11} - \bar{\lambda}\bar{\Omega} V_{22} = -5\bar{\eta} \left[\bar{\lambda} \left(\frac{V_{1;2}}{\alpha^2} + V_{2;1} \right) - \frac{\bar{\Omega}f}{2} \left(V_{11} - \frac{V_{22}}{\alpha^2} \right) \right] - \frac{8\alpha\beta(1+\beta^2)}{75} \bar{t}_c^5 \left[16\bar{\Omega}^5 \frac{\alpha^2 - 1}{1+\beta^2} V_{22} + (\bar{\lambda}^5 - 2\phi_1(\bar{\lambda}, \bar{\Omega}))V_{12} + \phi_2(\bar{\lambda}, \bar{\Omega})(V_{11} - V_{22}) \right], \quad (\text{B13})$$

$$\bar{\lambda}^2 V_{2;1} + \frac{\bar{\Omega}\bar{\lambda}f}{1+\alpha^2} V_{22} + \bar{\lambda}\bar{\Omega} V_{11} = -5\bar{\eta} \left[\bar{\lambda} \left(\frac{V_{1;2}}{\alpha^2} + V_{2;1} \right) - \frac{\bar{\Omega}f}{2} \left(V_{11} - \frac{V_{22}}{\alpha^2} \right) \right] - \frac{8\alpha\beta(\alpha^2 + \beta^2)}{75} \bar{t}_c^5 \left[16\bar{\Omega}^5 \frac{\alpha^2 - 1}{\alpha^2 + \beta^2} V_{11} + (\bar{\lambda}^5 - 2\phi_1(\bar{\lambda}, \bar{\Omega}))V_{12} + \phi_2(\bar{\lambda}, \bar{\Omega})(V_{11} - V_{22}) \right], \quad (\text{B14})$$

for $V_{i;j}$ even in index 3, and for those odd in index 3

$$\bar{\lambda}^2 V_{1;3} - 2\bar{\lambda}\bar{\Omega} V_{2;3} - \frac{\alpha^2 \bar{\Omega}^2 f^2}{(1+\alpha^2)^2} V_{3;1} - \frac{2\alpha^2 \bar{\Omega}^2 f}{1+\alpha^2} V_{3;1} = (\bar{\Omega}^2 - 2\bar{B}_{13})V_{13} - 5\bar{\lambda}\bar{\eta} \left(\frac{V_{1;3}}{\beta^2} + V_{3;1} \right) - \frac{8\alpha\beta(1+\alpha^2)}{75} \bar{t}_c^5 \bar{\lambda}^5 V_{13} - \frac{128\alpha\beta(\alpha^2 - 1)}{75} \bar{t}_c^5 \bar{\Omega}^5 V_{23}, \quad (\text{B15})$$

$$\bar{\lambda}^2 V_{2;3} + 2\bar{\lambda}\bar{\Omega} V_{1;3} - \frac{\alpha^2 \bar{\Omega}^2 f^2}{(1+\alpha^2)^2} V_{3;2} - \frac{2\bar{\Omega}^2 f}{1+\alpha^2} V_{3;2} = (\bar{\Omega}^2 - 2\bar{B}_{23})V_{23} - 5\bar{\eta} \left[\bar{\lambda} \left(\frac{V_{2;3}}{\beta^2} + \frac{V_{3;2}}{\alpha^2} \right) - \frac{\bar{\Omega}f}{1+\alpha^2} \left(V_{3;1} + \frac{\alpha^2}{\beta^2} V_{1;3} \right) \right] - \frac{8\alpha\beta(1+\alpha^2)}{75} \bar{t}_c^5 \bar{\lambda}^5 V_{23} - \frac{128\alpha\beta(\alpha^2 - 1)}{75} \bar{t}_c^5 \bar{\Omega}^5 V_{13}, \quad (\text{B16})$$

$$\bar{\lambda}^2 V_{3;1} + \frac{2\bar{\Omega}\bar{\lambda}f}{1+\alpha^2} V_{3;2} - \frac{\alpha^2 \bar{\Omega}^2 f^2}{(1+\alpha^2)^2} V_{3;1} = -2\bar{B}_{13} V_{13} - 5\bar{\lambda}\bar{\eta} \left(V_{3;1} + \frac{V_{1;3}}{\beta^2} \right) - \frac{8\alpha\beta(\alpha^2 + \beta^2)}{75} \bar{t}_c^5 \left([\bar{\lambda}^5 - \phi_1(\bar{\lambda}, \bar{\Omega})]V_{13} - \phi_2(\bar{\lambda}, \bar{\Omega})V_{23} \right), \quad (\text{B17})$$

$$\bar{\lambda}^2 V_{3;2} - \frac{2\alpha^2 \bar{\Omega}\bar{\lambda}f}{1+\alpha^2} V_{3;1} - \frac{\alpha^2 \bar{\Omega}^2 f^2}{(1+\alpha^2)^2} V_{3;2} = -2\bar{B}_{23} V_{23} - 5\bar{\eta} \left[\bar{\lambda} \left(\frac{V_{3;2}}{\alpha^2} + \frac{V_{2;3}}{\beta^2} \right) - \frac{\bar{\Omega}f}{1+\alpha^2} \left(V_{3;1} + \frac{\alpha^2}{\beta^2} V_{1;3} \right) \right] - \frac{8\alpha\beta(1+\beta^2)}{75} \bar{t}_c^5 \left([\bar{\lambda}^5 - \phi_1(\bar{\lambda}, \bar{\Omega})]V_{23} + \phi_2(\bar{\lambda}, \bar{\Omega})V_{13} \right), \quad (\text{B18})$$

where \bar{A}_{ij} and \bar{B}_{ij} are obtained from the index symbols A_{ij} and B_{ij} via the replacement $a_1 \rightarrow 1$, $a_2 \rightarrow \alpha = a_2/a_1$, $a_3 \rightarrow \beta = a_3/a_1$. Eqs. (B15)–(B16) can be simplified using Eq. (36)–(37) of Chap. 7 of EFE:

$$\bar{\Omega}^2 - Q_{12}Q_{21} + 2Q_{21}\bar{\Omega} = 2 \frac{a_1^2 - a_3^2}{a_1^2} \pi G\rho B_{13}, \quad (\text{B19})$$

$$\bar{\Omega}^2 - Q_{12}Q_{21} - 2Q_{12}\bar{\Omega} = 2 \frac{a_2^2 - a_3^2}{a_2^2} \pi G\rho B_{23}. \quad (\text{B20})$$

to obtain

$$\begin{aligned} \bar{\lambda}^2 V_{1;3} - 2\bar{\lambda}\bar{\Omega}V_{2;3} + 2\beta^2\bar{B}_{13}V_{3;1} &= (\bar{\Omega}^2 - 2\bar{B}_{13})V_{1;3} - 5\bar{\lambda}\bar{\eta}\left(\frac{V_{1;3}}{\beta^2} + V_{3;1}\right) - \frac{8\alpha\beta(1+\alpha^2)}{75}\bar{t}_c^5\bar{\lambda}^5 V_{13} \\ &\quad - \frac{128\alpha\beta(\alpha^2-1)}{75}\bar{t}_c^5\bar{\Omega}^5 V_{23}, \end{aligned} \quad (\text{B21})$$

$$\begin{aligned} \bar{\lambda}^2 V_{2;3} + 2\bar{\lambda}\bar{\Omega}V_{1;3} + \frac{2\beta^2}{\alpha^2}\bar{B}_{23}V_{3;2} &= (\bar{\Omega}^2 - 2\bar{B}_{23})V_{2;3} - 5\bar{\lambda}\bar{\eta}\left(\frac{V_{2;3}}{\beta^2} + \frac{V_{3;2}}{\alpha^2}\right) - \frac{8\alpha\beta(1+\alpha^2)}{75}\bar{t}_c^5\bar{\lambda}^5 V_{23} \\ &\quad - \frac{128\alpha\beta(\alpha^2-1)}{75}\bar{t}_c^5\bar{\Omega}^5 V_{13}. \end{aligned} \quad (\text{B22})$$

APPENDIX C: GRAVITATIONAL RADIATION BACK-REACTION TERM IN VIRIAL EQUATION 2: FULL 2.5-POST-NEWTONIAN FORM

Our derivation is similar, but more general, than that of Chandrasekhar (1970). In the rest frame of the center of mass, the radiation reaction terms in the equations of motion are (Chandrasekhar & Esposito 1970)

$$f_{\text{GW}}^a = \frac{1}{c}T^{aj}_{;j} = \frac{1}{c^5}\left[-\rho Q_{00}^{(5)}\frac{dv_a}{dt} - \frac{1}{2}\rho v_a\frac{dQ_{00}^{(5)}}{dt} - \rho\frac{d}{dt}\left(v_i Q_{ia}^{(5)}\right) - \frac{1}{2}\rho Q_{ij}^{(5)}\frac{d\mathfrak{B}_{ij}}{dx_a} + \frac{1}{5}\rho x_a G\frac{d^5 I_{ii}}{dt^5} - \frac{3}{5}\rho x_i G\frac{d^5 I_{ia}}{dt^5}\right], \quad (\text{C1})$$

where the Einstein summation convention is used. The Latin indices that are not explicitly summed over run over the spatial indices 1,2,3. v_a is the velocity as measured in the inertial frame. $Q_{00}^{(5)}$ and $Q_{ab}^{(5)}$ are given by

$$Q_{00}^{(5)} = \frac{4}{3}G\frac{d^3 I_{ii}}{dt^3}, \quad (\text{C2})$$

$$Q_{ab}^{(5)} = 2G\frac{d^3 I_{ab}}{dt^3} - \frac{2}{3}G\delta_{ab}\frac{d^3 I_{ii}}{dt^3}, \quad (\text{C3})$$

where I_{ab} is the moment of inertia as measured in the inertial frame (although Chandrasekhar (1970) does not explicitly state this) and \mathfrak{B}_{ij} is defined in Eq. (12).

In the frame rotating with the star about the x_3 axis, which is the same in both rotating and inertial frames, the moment of inertia tensor $I_{ab}^{(r)}$ is constant and diagonal

$$I_{ab}^{(r)} = \int_{\mathcal{V}} d^3x \rho x_a x_b = \delta_{ab} I_{aa}. \quad (\text{C4})$$

The time derivatives of the moment of inertia tensor in the inertial frame, $I_{ab}^{(i)}$, are related to those of $I_{ab}^{(r)}$ by Eq. (14) of Chandrasekhar (1970):

$$\frac{d^n I_{ab}^{(i)}}{dt^n} = \sum_{m=0}^n \sum_{p=0}^m C_m^n C_p^m (-1)^p [(\mathbf{\Omega}^*)^p]_{abc} \frac{d^{n-m} I_{ck}^{(r)}}{dt^{n-m}} [(\mathbf{\Omega}^*)^{m-p}]_{kb} = \Omega^n \sum_{p=0}^n C_p^n (-1)^p [\sigma^p]_{ac} I_{ck}^{(r)} [\sigma^{n-p}]_{kb}, \quad (\text{C5})$$

where σ_{ab} is

$$\sigma_{ab} = \begin{pmatrix} 0 & 1 & 0 \\ -1 & 0 & 0 \\ 0 & 0 & 0 \end{pmatrix}. \quad (\text{C6})$$

From Eq. (C5), one finds (Chandrasekhar (1970) Eq. (18))

$$\frac{d^{2n+1} I_{ab}^{(i)}}{dt^{2n+1}} = (-1)^n 2^{2n} \Omega^{2n+1} (I_{11} - I_{22}) \begin{pmatrix} 0 & 1 & 0 \\ 1 & 0 & 0 \\ 0 & 0 & 0 \end{pmatrix}. \quad (\text{C7})$$

So $Q_{00}^{(5)} = 0$ and $d^5 I_{ab}^{(i)}/dt^5 = 0$ are still true as in Chandrasekhar (1970), but their perturbations are not necessarily zero.

We are also going to be concerned with the perturbed form of this when we compute the contribution of gravitational radiation back-reaction to the second-order virial equation. Noting that

$$\delta I_{ab}^{(r)} = \int_{\mathcal{V}} d^3x \rho (\xi_a x_b + x_a \xi_b), \quad (\text{C8})$$

and assuming (as in the main text) $\xi_i(\mathbf{x}, t) = e^{\lambda t} \xi_i(\mathbf{x})$, we have

$$\frac{d^{n-m} I_{ab}^{(r)}}{dt^{n-m}} = \lambda^{n-m} V_{ab}, \quad (\text{C9})$$

and hence the perturbation of the time derivatives of the inertial frame moment of inertia are

$$\delta I_{ab}^{(n)} \equiv \frac{d^n \delta I_{ab}^{(i)}}{dt^n} = \sum_{m=0}^n \sum_{p=0}^m \lambda^{n-m} \Omega^m C_m^n C_p^m (-1)^p [\sigma^P]_{ac} V_{ck} [\sigma^{m-p}]_{kb}. \quad (\text{C10})$$

Chandrasekhar (1970) often uses the abbreviation $\delta I_{ab}^{(n)}$, and so do we to be able to compare to his results for Maclaurin spheroid. The forms of this tensor for $n = 3, 4, 5$ are given by Chandrasekhar (1970) Eq. (26)–(28).

We also need the background velocity v_a and acceleration dv_a/dt , which in the Riemann S-type ellipsoid case are

$$v_a = u_a + \varepsilon_{abi} \Omega_b x_i \equiv \Omega \tilde{S}_{ab} x_b, \quad (\text{C11})$$

$$\frac{dv_a}{dt} = \frac{du_a}{dt} + \varepsilon_{abi} \Omega_b \varepsilon_{icj} \Omega_c x_j + 2\varepsilon_{abi} \Omega_b u_i = -\Omega^2 \tilde{R}_a x_a, \quad (\text{C12})$$

where u_a is the background velocity in the rotating frame defined in Eq. (5)–(7). This can be compared to Eq. (31) in Chandrasekhar (1970) where in the Maclaurin ellipsoid case the vorticity is zero so $u_a = 0$. The nonzero \tilde{S}_{ab} are

$$\tilde{S}_{12} = -1 - \frac{a_1^2 f}{a_1^2 + a_2^2}, \quad \tilde{S}_{21} = 1 + \frac{a_2^2 f}{a_1^2 + a_2^2}, \quad (\text{C13})$$

and the nonzero \tilde{R}_a are

$$\tilde{R}_1 = 1 + \frac{a_2^2 f}{a_1^2 + a_2^2} + \frac{a_1^2 a_2^2 f^2}{(a_1^2 + a_2^2)^2}, \quad \tilde{R}_2 = 1 + \frac{a_1^2 f}{a_1^2 + a_2^2} + \frac{a_1^2 a_2^2 f^2}{(a_1^2 + a_2^2)^2}, \quad (\text{C14})$$

and $v_3 = 0 = dv_3/dt$.

Taking the perturbation of Eq. (C1) and using that $Q_{00}^{(5)} = 0$, $d^5 I_{ab}^{(i)}/dt^5 = 0$, we find

$$\begin{aligned} \delta f_{\text{GW}}^a &= \frac{1}{c^5} \delta \left[-\rho \frac{dv_i}{dt} Q_{ia}^{(5)} - \rho v_i \frac{dQ_{ia}^{(5)}}{dt} - \frac{1}{2} \rho Q_{ij}^{(5)} \frac{d\mathfrak{B}_{ij}}{dx_a} - \frac{3}{5} \rho x_i G \frac{d^5 I_{ia}}{dt^5} \right] \\ &= \frac{1}{c^5} \left[-\rho \frac{d\delta v_i}{dt} Q_{ia}^{(5)} - \rho \delta v_i \frac{dQ_{ia}^{(5)}}{dt} - \rho \frac{dv_i}{dt} \delta Q_{ia}^{(5)} - \rho v_i \frac{d\delta Q_{ia}^{(5)}}{dt} - \frac{1}{2} \rho \delta Q_{ij}^{(5)} \frac{d\mathfrak{B}_{ij}}{dx_a} - \frac{1}{2} \rho Q_{ij}^{(5)} \frac{d\delta \mathfrak{B}_{ij}}{dx_a} \right. \\ &\quad \left. - \frac{3}{5} \rho \delta x_i G \frac{d^5 I_{ia}}{dt^5} - \frac{3}{5} \rho x_i G \frac{d^5 \delta I_{ia}}{dt^5} - \rho \delta Q_{00}^{(5)} \frac{dv_a}{dt} - \frac{1}{2} \rho v_a \frac{d\delta Q_{00}^{(5)}}{dt} + \frac{1}{5} \rho x_a G \frac{d^5 \delta I_{ii}}{dt^5} \right]. \end{aligned} \quad (\text{C15})$$

The contribution to the second-order virial equation, denoted $\delta \mathcal{G}_{ij}$ in Eq. (2), is

$$\delta \mathcal{G}_{ab} = \int_{\mathcal{V}} d^3 x x_b \delta f_a^{\text{GW}}. \quad (\text{C16})$$

Using that $\delta x_i = \xi_i$, the eight terms on the right-hand side of this are thus (labeled with a superscript number in brackets)

$$\delta \mathcal{G}_{ab}^{(1)} \equiv -\frac{1}{c^5} \int_{\mathcal{V}} d^3 x \left[\rho x_b \frac{d\delta v_i}{dt} Q_{ia}^{(5)} \right] = \frac{\Omega^2}{c^5} \int_{\mathcal{V}} d^3 x \left[\rho x_b \tilde{R}_i \xi_i Q_{ia}^{(5)} \right] = -\frac{8G\Omega^5}{c^5} (I_{11} - I_{22}) \left(\tilde{R}_1 \delta_a^2 V_{1;b} + \tilde{R}_2 \delta_a^1 V_{2;b} \right) \quad (\text{C17})$$

$$\begin{aligned} \delta \mathcal{G}_{ab}^{(2)} &\equiv -\frac{1}{c^5} \int_{\mathcal{V}} d^3 x \left[\rho x_b \delta v_i \frac{dQ_{ia}^{(5)}}{dt} \right] = -\frac{\Omega}{c^5} \int_{\mathcal{V}} d^3 x \left[\rho x_b \left(\tilde{S}_{21} \delta_a^2 \xi_1 + \tilde{S}_{12} \delta_a^1 \xi_2 \right) \frac{dQ_{ia}^{(5)}}{dt} \right] = \\ &= -\frac{16G\Omega^5}{c^5} (I_{11} - I_{22}) \left(\tilde{S}_{12} \delta_a^1 V_{2;b} - \tilde{S}_{21} \delta_a^2 V_{1;b} \right), \end{aligned} \quad (\text{C18})$$

where we used Eq. (17) of Chandrasekhar (1970),

$$\frac{d^{2n} I_{ab}^{(i)}}{dt^{2n}} = (-1)^n 2^{2n-1} \Omega^{2n} (I_{11} - I_{22}) \begin{pmatrix} 1 & 0 & 0 \\ 0 & -1 & 0 \\ 0 & 0 & 0 \end{pmatrix}_{ab}, \quad (\text{C19})$$

$$\begin{aligned} \delta \mathcal{G}_{ab}^{(3)} &\equiv -\frac{1}{c^5} \int_{\mathcal{V}} d^3 x \left[\rho x_b \frac{dv_i}{dt} \delta Q_{ia}^{(5)} \right] = \frac{2G\Omega^2}{c^5} \int_{\mathcal{V}} d^3 x \left[\rho x_b \left(\tilde{R}_1 x_1 \delta_i^1 + \tilde{R}_2 x_2 \delta_i^2 \right) \delta Q_{ia}^{(5)} \right] \\ &= \frac{2G\Omega^2}{c^5} \left[I_{11} \tilde{R}_1 \delta_b^1 \left(\delta I_{1a}^{(3)} - \frac{1}{3} \delta_{1a} \delta I_{jj}^{(3)} \right) + I_{22} \tilde{R}_2 \delta_b^2 \left(\delta I_{2a}^{(3)} - \frac{1}{3} \delta_{2a} \delta I_{jj}^{(3)} \right) \right], \end{aligned} \quad (\text{C20})$$

where we used that the moment of inertia tensor in the rotating frame is diagonal i.e. Eq. (C4),

$$\delta \mathcal{G}_{ab}^{(4)} \equiv -\frac{1}{c^5} \int_{\mathcal{V}} d^3 x \left[\rho x_b v_i \frac{d\delta Q_{ia}^{(5)}}{dt} \right] = -\frac{2G\Omega}{c^5} \left[I_{11} \tilde{S}_{21} \delta_b^1 \left(\delta I_{2a}^{(4)} - \frac{1}{3} \delta_{2a} \delta I_{jj}^{(4)} \right) + I_{22} \tilde{S}_{12} \delta_b^2 \left(\delta I_{1a}^{(4)} - \frac{1}{3} \delta_{1a} \delta I_{jj}^{(4)} \right) \right], \quad (\text{C21})$$

$$\delta\mathcal{G}_{ab}^{(5)} \equiv -\frac{1}{2c^5} \int_{\mathcal{V}} d^3x \rho x_b \delta Q_{ij}^{(5)} \frac{d\mathfrak{B}_{ij}}{dx_a} = -\frac{4G(\pi G\rho)}{c^5} \left[B_{ab} I_{bb} \left(\delta I_{ab}^{(3)} - \frac{1}{3} \delta_{ab} \delta I_{jj}^{(3)} \right) - \frac{1}{3} a_i^2 \delta_{ab} I_{aa} A_{ia} \delta I_{ii}^{(3)} \right], \quad (\text{C22})$$

where we used

$$\frac{d\mathfrak{B}_{ij}}{dx_a} = \pi G\rho \left[2B_{ij} (x_j \delta_i^a + x_i \delta_j^a) - 2a_i^2 \delta_{ij} A_{ia} x_a \right], \quad (\text{C23})$$

$$\delta\mathcal{G}_{ab}^{(6)} \equiv -\frac{1}{2c^5} \int_{\mathcal{V}} d^3x \rho x_b Q_{ij}^{(5)} \frac{d\delta\mathfrak{B}_{ij}}{dx_a} = \frac{16G(\pi G\rho)\Omega^3}{c^5} B_{12} (I_{11} - I_{22}) \left(\delta_a^2 V_{1;b} + \delta_a^1 V_{2;b} \right), \quad (\text{C24})$$

where we used

$$\frac{d\delta\mathfrak{B}_{ij}}{dx_a} = \pi G\rho \left[2B_{ij} (\xi_j \delta_i^a + \xi_i \delta_j^a) - 2a_i^2 \delta_{ij} A_{ia} \xi_a \right], \quad (\text{C25})$$

$$\delta\mathcal{G}_{ab}^{(7)} \equiv -\frac{3}{5c^5} \int_{\mathcal{V}} d^3x \rho x_b \delta x_i G \frac{d^5 I_{ia}}{dt^5} = -\frac{48G\Omega^5}{5c^5} B_{12} (I_{11} - I_{22}) \left(\delta_a^2 V_{1;b} + \delta_a^1 V_{2;b} \right), \quad (\text{C26})$$

$$\delta\mathcal{G}_{ab}^{(8)} \equiv -\frac{3}{5c^5} \int_{\mathcal{V}} d^3x \rho x_b x_i G \frac{d^5 \delta I_{ia}}{dt^5} = -\frac{3G}{5c^5} I_{bb} \delta I_{ba}^{(5)}, \quad (\text{C27})$$

$$\delta\mathcal{G}_{ab}^{(9)} \equiv -\frac{1}{c^5} \int_{\mathcal{V}} d^3x \rho x_b \delta Q_{00}^{(5)} \frac{dv_a}{dt} = \frac{4G\Omega^2}{c^5} \left(I_{11} \tilde{R}_1 \delta_a^1 \delta_b^1 + I_{22} \tilde{R}_2 \delta_a^2 \delta_b^2 \right) \delta I_{ii}^{(3)}, \quad (\text{C28})$$

$$\delta\mathcal{G}_{ab}^{(10)} \equiv -\frac{1}{2c^5} \int_{\mathcal{V}} d^3x \rho x_b v_a \frac{d\delta Q_{00}^{(5)}}{dt} = -\frac{2G\Omega}{3c^5} \left(I_{11} \tilde{S}_{21} \delta_a^2 \delta_b^1 + I_{22} \tilde{S}_{12} \delta_a^1 \delta_b^2 \right) \delta I_{ii}^{(4)}, \quad (\text{C29})$$

$$\delta\mathcal{G}_{ab}^{(11)} \equiv \frac{1}{5c^5} \int_{\mathcal{V}} d^3x \rho x_b x_a G \frac{d^5 \delta I_{ii}}{dt^5} = \frac{G}{5c^5} I_{bb} \delta_{ab} \delta I_{ii}^{(5)}. \quad (\text{C30})$$

In the case of Maclaurin spheroid discussed in Chandrasekhar (1970), $a_1 = a_2$ and so $I_{11} = I_{22}$, in which case many of the contributions to $\delta\mathcal{G}_{ab}$ are eliminated. If we also discard the V_{ab} with either of the indices being equal 3, the remaining terms reproduce Eq. (35)–(38) of Chandrasekhar (1970).

This paper has been typeset from a $\text{\TeX}/\text{\LaTeX}$ file prepared by the author.